AMMRC TR 70-32

AD

DYNAMIC RESPONSE OF A CONSTRAINED FIBROUS SYSTEM SUBJECTED TO TRANSVERSE IMPACT Part I - TRANSIENT RESPONSES AND BREAKING ENERGIES OF NYLON YARNS

ANTHONY E. WILDE, JOHN J. RICCA,
LONNIE M. COLE, and JOSEPH M. ROGERS
FIBERS AND POLYMERS DIVISION

November 1970

ARMY MATERIALS AND MECHANICS RESEARCH CENTER
Watertown, Massachusetts 02172

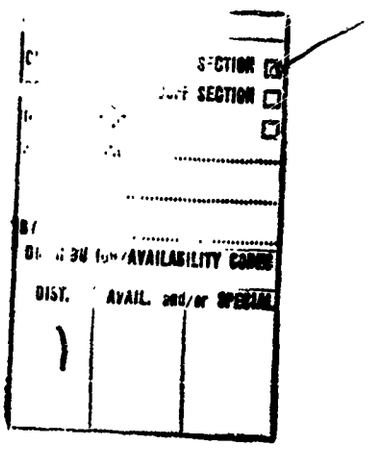

The findings in this report are not to be construed as an official Department of the Army position, unless so designated by other authorized documents.

Mention of any trade names or manufacturers in this report shall not be construed as advertising nor as an official indorsement or approval of such products or companies by the United States Government.

DISPOSITION INSTRUCTIONS

Destroy this report when it is no longer needed.
Do not return it to the originator.

AMMRC TR 70-32

DYNAMIC RESPONSE OF A CONSTRAINED FIBROUS SYSTEM SUBJECTED TO TRANSVERSE IMPACT. Part I. TRANSIENT RESPONSES AND BREAKING ENERGIES OF NYLON YARNS.

Technical Report by

ANTHONY F. WILDE, JOHN J. RICCA, LONNIE M. COLE, and JOSEPH M. ROGERS

November 1970

D/A Project 1T062105A329
AMCMS Code 502E.11.295
Organic Materials Research for Army Materiel
Agency Accession Number DA OB4752

FIBERS AND POLYMERS DIVISION
ARMY MATERIALS AND MECHANICS RESEARCH CENTER
Watertown, Massachusetts 02172

ARMY MATERIALS AND MECHANICS RESEARCH CENTER

DYNAMIC RESPONSE OF A CONSTRAINED FIBROUS SYSTEM SUBJECTED TO TRANSVERSE IMPACT

PART I: TRANSIENT RESPONSES AND BREAKING ENERGIES OF NYLON YARNS

ABSTRACT

The transverse deformation and rupture of yarns under high-speed missile impact is being studied to gain a better understanding of the ballistic performance of textile materials. A specially designed guided projectile transverse impacter has been constructed. This system restrains the motion of the missile and yarn to a single plane and allows high-speed photographs to be taken of the entire sequence of events. The first phase of the program has been concerned with direct determination of the loss in missile kinetic energy occurring during the yarn deformation and rupture processes. This was calculated from the reduction in missile velocity which was obtained from a series of flash photographs taken at time intervals ranging from 50 to 1700 microseconds.

Four commercial nylon 6/6 yarns were studied, providing a series with graded mechanical properties, ranging in tenacity from 1.00 to 8.45 grams per denier. Impact velocities ranged from 25 to 420 meters per second, corresponding roughly to strain rates of 3×10^5 to 6×10^6 percent per minute. For each yarn, the loss in missile energy increased with missile impact velocity to a maximum value and then decreased rapidly toward zero. Comparisons made with the four yarns showed that these energy loss envelopes increased monotonically with yarn tenacity both in energy magnitude and velocity range. Also the peak values of missile energy loss showed opposite tenacity dependence from the static breaking energies obtained by Instron testing. The estimated breaking strains under impact for these yarns were all less than their static values and, with one exception, were roughly the same for all yarns, in contrast to their widely differing static values. From the photographs estimates were also made of the missile travel distance and transverse wave travel distance at break.

Subsequent analysis showed that the loss in missile kinetic energy is converted into both yarn kinetic energy and yarn strain energy. The yarn kinetic energy term goes through a peak as a function of missile impact velocity because of constraints at the clamped ends of the yarn specimen, thus causing the observed peak in the total energy loss envelopes. Consideration of both the impact velocity at these peak values (kinetic energy term) and the estimated breaking strains for the impact tests (strain energy term) provided an explanation for the opposite tenacity dependences mentioned above. Each of these energy loss envelopes for the yarns was somewhat similar in shape to actual ballistic energy loss versus velocity relationships reported for nylon felts. For the high-tenacity yarn, the breaking strain energy component at high-speed impact was estimated and then compared to the breaking energy obtained directly at lower strain rates. This comparison indicated that the strain energy to break for this nylon yarn goes through a minimum at intermediate strain rates, in general agreement with trends deduced from data reported by others. All of this suggests that yarn behavior observed at low rates may have little significance for yarn response at ballistic rates of deformation.

FOREWORD

Although at low areal densities textiles offer a very respectable ballistic performance, there is a continuing need to improve still further the degree of protection furnished by textile materials against the threat of bullets and fragments. This requires more knowledge of details of the transient behavior of the component elements of textile structures during high-speed impact, particularly over a range of impact velocites or strain rates. The work described in this report was undertaken to develop techniques suitable for such an investigation and to provide data concerning the dynamic response of constrained yarn specimens.

The authors wish to express their appreciation to various persons in the AMMRC machine shop for their interest and skill in the construction of the Guided Projectile Transverse Impacter and the projectiles from the detailed designs furnished by the authors.

The work for this program was performed under Department of the Army Project 1F162203A150 in FY 69 and Project 1T062105A329 in FY 70.

CONTENTS

I. INTRODUCTION

The purpose of this program is to acquire a better understanding of the various factors which determine the ballistic performance of textile materials. The first step has been to develop techniques suitable for a scientific investigation on a laboratory scale of the transient responses of textile materials to high-speed mechanical impact. Small textile elements, namely yarns, were chosen for study because of their simplicity and their availability in a variety of chemical types and mechanical properties. Exploratory efforts indicated that multiple-exposure microflash photography provided a way to follow the deformation process from impact to rupture, and, in combination with a recently developed pneumatic impacter, could yield direct measurements of the projectile kinetic energy loss resulting from the deformation and rupture of the yarn specimen.

In recent years, studies of the high-speed deformation of single yarns have been conducted by other groups of investigators. For example, tension testing at velocities up to 18.3 ft/sec has been done by Dogliotti and Yelland,[1] and at velocities up to 20 meter/sec by Hall.[2] Pilsworth[3] has studied the longitudinal impact of yarns at velocities of 150 ft/sec. Transverse impacts upon yarns have been conducted by Petterson et al.[4,5] at velocities up to 1900 ft/sec, and by Smith et al.[6-9] at velocities up to 725 meter/sec. The principal purpose of these studies has been the derivation of stress-strain curves appropriate to the conditions under which the material was tested.

It was felt by our group at AMMRC that the quantity probably most closely related to ballistic performance would be the energy-absorbing capability of the target material. A good index of this quantity, and one for which we had developed a laboratory technique, involves the measurement of the projectile kinetic energy loss resulting from its interaction with the target material. Another motivating factor in our approach has been the desire to relate the high-speed yarn behavior to specific material properties. This requires that a study be made of a series of materials varying systematically in only one selected property, with all other properties kept constant. Therefore, we established a program believed to be unique in that it combined three important factors: (a) transverse impact at high velocities, (b) with direct measurement of the projectile kinetic energy loss, and (c) for a series of chemically identical yarns differing systematically in tenacity. We have thus undertaken an integrated experimental program which involves a direct and materials-oriented approach toward an improved understanding of the ballistic performance of textile materials.

This report will describe the first stages of work performed under this program, including descriptions of the yarns which were studied, the instrumentation and techniques which were developed, and the results obtained to date concerning various aspects of the transient behavior of the impacted yarns.

II. DESCRIPTION AND STATIC TESTING OF NYLON YARNS

A. Description

A series of four commercial nylon 6/6 yarns was chosen for study. These four yarns provide a series with graded mechanical properties. The actual values of

denier* were measured by the manufacturer; the tenacity† and percent elongation-to-break and initial modulus values were taken from the longitudinal single-yarn stress-strain curves supplied by the manufacturer. See Figure 1 for typical curves. The energy-to-break was computed at AMMRC from these stress-strain curves. The molecular weight data are the manufacturer's. The yarns and their properties are listed in Table I. The dependences of elongation-to-break and energy-to-break upon the tenacity are shown graphically in Figure 2 (static longitudinal properties only).

Table I. PROPERTIES OF FOUR SELECTED COMMERCIAL NYLON 6/6 YARNS

Yarn Code	Yarn Category	Molecular Weight	Den/Fil (Nominal)	Actual Denier	Twist*	Tenacity, g/den	Elongation-to-Break, %	Initial Modulus, g/den	Energy-to-Break, Joule/g
A	Tire	20,000	840/140	863	0.5Z	8.45	17.6	53.2	81
B	Textile	15,000	70/34	71.4	0.5Z	5.05	24.9	45.2	104
C	Texturized Carpet	17,200	2500/136	2685	0.5S	2.69	67.8	6.5	131
D	Undrawn	17,500	-/34	1031	--	1.00	379	7.2	211

*Twist is specified by the number of turns per inch and the direction of the twist. For instance 0.5Z means 0.5 turns per inch in the right-handed direction, and 0.5S means 0.5 turns per inch in the left-handed direction.

B. Static Testing

1. Purpose, Apparatus, and Procedure

Samples of the same series of nylon 6/6 yarns were subjected to static (Instron) testing, both longitudinal and transverse, to determine the following:

a. how closely the manufacturer's longitudinal stress-strain results could be reproduced at AMMRC;

b. comparisons of the breaking energy for transverse and longitudinal static tests; and

c. the relationships between breaking energy for static tests and transverse impact tests.

The Instron machine was a Type TT-C1 floor model. Type 4C pneumatic cord and yarn grips were used. The conditions for the longitudinal static tests

*Denier: A measure of the linear density expressed as the weight in grams per 9000-meter length.

†Tenacity: A measure of the ultimate tensile strength, expressed as the breaking force per unit linear density, in units of grams per denier. To convert from g/den to psi, multiply by 12,800 · density, where density is in g/cm^3.

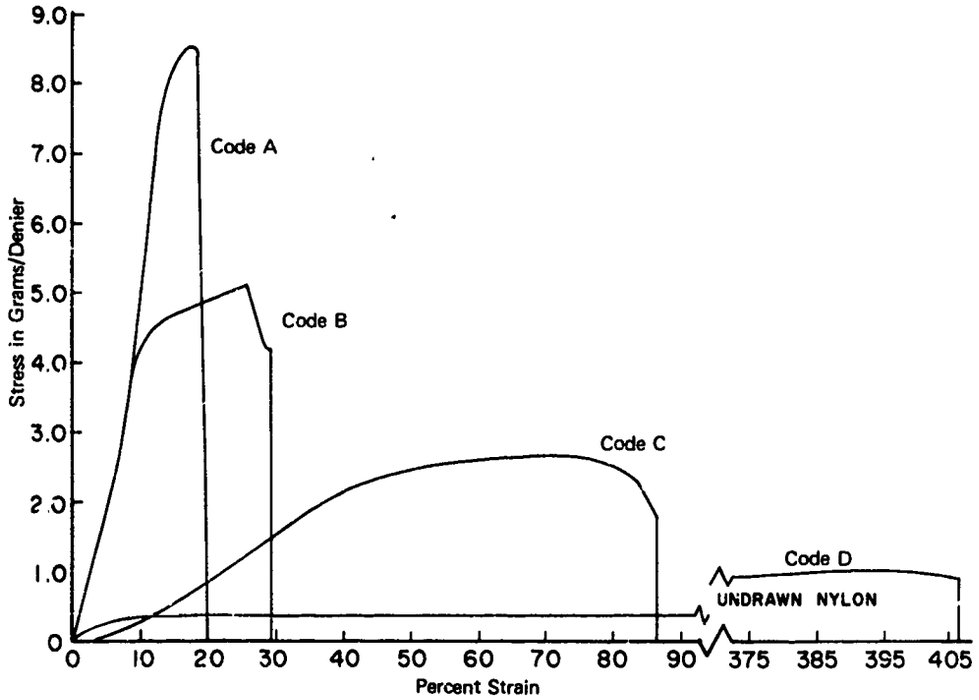

Figure 1. Longitudinal single-yarn stress-strain curves for the four nylon 6/6 yarns

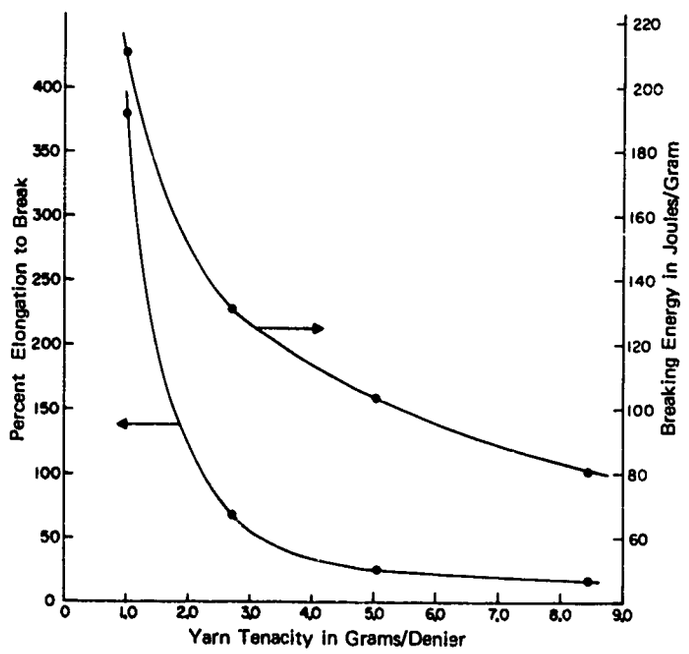

Figure 2. Static longitudinal properties of nylon 6/6 yarns as a function of yarn tenacity. Data taken from manufacturer's stress-strain curves

performed at AMMRC were chosen to duplicate those used by the manufacturer, namely, gage length 10 inches, crosshead speed 12 in./min (thus strain rate was 120 percent/min) for all yarns except the undrawn nylon. For this yarn, the manufacturer's tests used a gage length of 5 inches and a crosshead speed of 12 in./min (thus strain rate was 240 percent/min). For the undrawn nylon, the AMMRC tests used the same crosshead speed but a shorter gage length (2.1 or 4.1 inches, thus strain rate was 570 percent/min or 290 percent/min) to ensure complete yarn breakage within the available crosshead travel distance, see Table II.

Table II. CONDITIONS FOR STATIC TESTING

Tested by	Yarn	Gage Length, in.	Speed, in./min		Strain Rate, %/min
			Crosshead	Crossarm	
Longitudinal					
Mfr	All but undrawn nylon	10	12		120
	Undrawn nylon	5	12		240
AMMRC	All but undrawn nylon	10	12		120
	Undrawn nylon	2.1 or 4.1	12		570 or 290
Transverse					
AMMRC	All but undrawn nylon	12		12	See Table III
	Undrawn nylon	4		12	See Table III

The transverse static tests were performed at AMMRC. A fixture was specially designed and built to hold the yarn specimen in a horizontal position. This fixture was attached to the lower (movable) crossarm of the Instron and moved downward during the test. A slotted bar holding a standard missile (to be described in Section IIIA) was suspended vertically from the upper crosshead. The yarn specimen passed through the slotted bar and over the impact face of the missile. The ends of the yarn were held in flat-faced clamps with rounded edges. During the test the yarn moved downward while the missile remained stationary. The force on the missile (at the apex of the growing yarn cone) was obtained from the load cell in the usual way and was recorded on the strip chart along with the lower crossarm travel distance. These tests used a gage length of 12 inches, for all yarns except the undrawn nylon, to duplicate the 12-inch length of the samples to be impacted transversely. The undrawn nylon gage length was 4 inches, again to permit complete yarn breakage for this highly extensible yarn. The crossarm speed for all the transverse static tests was 12 in./min, see Table II.

For the transverse static tests, it must be noted that the strain rate is not constant in spite of the constant crossarm speed, due to the changing dimensions of the triangle formed by the stretching yarn. The strain rate increases monotonically during the course of the test according to the equation

$$\text{Strain rate} = \frac{x}{l_0\sqrt{l_0^2 + x^2}} \frac{dx}{dt} \qquad (1)$$

where l_0 is one half the original yarn length, x is the crossarm travel distance, and dx/dt is the crossarm speed. Typical strain rates are shown in Table III for the two-gage lengths used in these transverse tests. Values of strain are also included for comparative purposes.

From analyses performed at AMMRC, it was determined that for the transverse static tests, the energy-to-break could be computed simply by integration of the force-distance curve obtained from the Instron. Accordingly, this was done for the transverse test data.

Table III. TRANSVERSE STATIC TESTING AT 12 INCHES/MINUTE

Crossarm Travel Distance, in.	Gage Length			
	12-Inch		4-Inch	
	Strain, %	Strain Rate, %/min	Strain, %	Strain Rate, %/min
0	0	0	0	0
1	1.4	33	12	268
2	5.4	63	41	424
3	12	89	80	499
4	20	111	124	537
5	30	128	169	557
6	41	141	216	570
7	54	152	264	577
8	67	160	312	582
10	94	171	410	588
12	124	179	508	592
∞	∞	200	∞	600

2. Experimental Results

The breaking energy data for the static tests appear in Table IV. It is seen that for both types of static tests, the AMMRC energy data change with yarn type in the same way as do the manufacturer's data (breaking energy increases with decreasing yarn tenacity as in Figure 2).

Comparisons between various tests for each yarn are also made in Table IV. The ratio numbers refer to the purposes mentioned in the beginning of Section IIB. Ratio 1: It is seen that the AMMRC longitudinal tests absorbed somewhat less energy than the manufacturer's tests, except for the undrawn nylon. Ratio 2: The transverse static tests absorbed considerably less energy than the longitudinal tests, again except for the undrawn nylon.

We do not know at this point what are the theoretical relationships between the longitudinal and transverse types of tests or if they might be entirely equivalent. However, it appears that the transverse test specimens would be subjected to a greater degree of stress concentrations at the clamps than would the longitudinal specimens because of the smaller radii of curvature at the edges of the flat-faced clamps compared with the pneumatic grips used for the longitudinal tests. In addition, there would be stress concentrations at the center of the transverse test specimen in the region where it contacts the missile face. The net effect would be that the transverse test specimens would undergo premature

Table IV. BREAKING ENERGY DATA PER MASS YARN IN JOULES/GRAM

Yarn Code	Yarn Tenacity, g/den	Static Test, 1 Yarn				
		Longitudinal		Transverse	Ratios, %*	
		Mfr	AMMRC	AMMRC	1	2
A	8.45	81 ($\frac{86}{76}$)	62 ($\frac{74}{57}$)	39 ($\frac{46}{33}$)	77	63
B	5.05	104 ($\frac{118}{86}$)	99 ($\frac{108}{93}$)	65 ($\frac{82}{35}$)	95	66
C - Texturized	2.69	131 ($\frac{139}{121}$)	125 ($\frac{134}{118}$)	83 ($\frac{93}{77}$)	95	66
D - Undrawn	1.00	211 ($\frac{219}{202}$)	266 ($\frac{275}{252}$)	287 ($\frac{313}{211}$)	126	108

*Ratio 1 - Longitudinal: AMMRC/Mfr
Ratio 2 - AMMRC: Transverse/Longitudinal

Figures in parentheses show spread of values

failure and thus absorb less energy. This is confirmed by a comparison of the approximate breaking strains observed for both types of tests and which are listed in Table V. (The values for the transverse tests are only very approximate because of the asymptotic nature of the beginning of the curve on the strip chart.) It is seen that the transverse test specimens did have lower breaking strains for all except the undrawn nylon. It is notable that the transverse/longitudinal ratio of breaking strains given in Table V varies with tenacity in the same way as the transverse/longitudinal ratio of breaking energies listed in Table IV, showing that the energies and strains are apparently closely related.

A further point to be made here involves the susceptibility of the yarns to failure by the creation of stress concentrations. If one considers that the ratios given in Table V are an inverse measure of the degree of premature failure

Table V. APPROXIMATE BREAKING STRAIN FOR STATIC TESTS DONE BY AMMRC

Yarn Code	Yarn Tenacity, g/den	Strain, %		$\frac{\text{Transverse}}{\text{Longitudinal}}$, %
		Longitudinal	Transverse (very approximate)	
A	8.45	17.3	7	40
B	5.05	30	15	50
C - Texturized	2.69	76	40	53
D - Undrawn	1.00	505	564	112

(the lower the ratio, the sooner the transverse failure), it is seen that the higher tenacity yarns are more prone to fail under the localized stress concentrations produced by the transverse tests. This seems reasonable in terms of the concept of brittle and ductile behavior, which might be represented to a fair degree by the value of yarn tenacity.

III. TRANSVERSE IMPACT TESTS

A. Instrumentation

1. Introduction

The transverse impact tester developed for this research study has the following features: (1) provides for the capability of testing materials in the form of thin strips or yarns under test conditions similar to those used in personnel armor evaluation testing; (2) provides for a considerable degree of control of experimental parameters such as pre-impact alignment of projectile and test material orientation of projectile face during impact time, and the type projectile impact face geometry; (3) constrains the projectile to linear motion and the yarn to motion in a plane during the test time, which in turn allows for improved precision of transverse wave measurements and projectile velocity measurements from high-speed photographic records of transverse impacts over a wide range of impact velocities; and (4) provides good potential for automating measurements of the projectile velocity before, during, and after the impact-to-break time. Commercial and research type of transverse impact testing instruments,[4,6,8,10] lack two or more of the above desired features.

It should be noted that the instrumentation described in this report reflects the first prototype and preliminary evaluation of the concept of this transverse impact tester.

2. Description and Operation of the Loading System and the High-Speed Photographic System

a. Loading System. The transverse impact tester consists of a pneumatic loading system and a high-speed photographic system shown in Figure 3.

The unique components of the loading system, designed by John J. Ricca, consist of a square cross section slotted projectile guide and projectile (see Figure 4). The device is called a "Guided Projectile Transverse (GPT) Impacter." The grooves in the projectile guide extend along its entire length and the rails of the projectile ride in these grooves. The projectile rails have a close-tolerance slide fit in the grooves and are the only part of the projectile which comes in contact with the projectile guide. The height of one of the extended sides of the projectile guide has been cut away so that a portion of the projectile extends above this side to allow for the photographing of the projectile during the impact time (see Figures 6 and 8 for typical photographs).

The geometrical configuration of the projectile used in all experiments, (with the exception of the work related to part (b), Projectile Impact Face Geometry presented in Section IIIA6), is shown in Figure 4. The projectiles in

19-066-76/AMC-70

Figure 3. Overall view of apparatus, including the GPT impacter, yarn specimen, and still camera

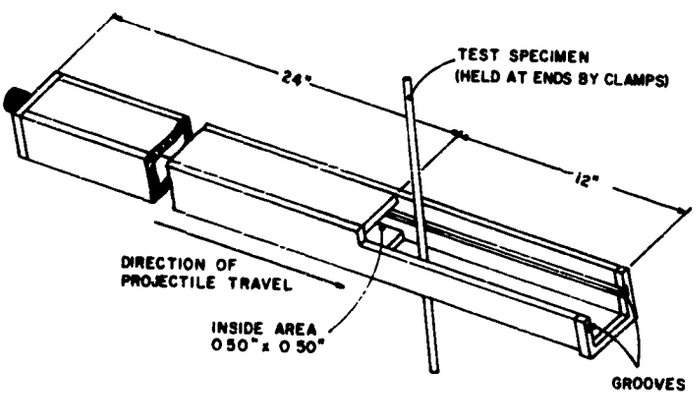

SLOTTED PROJECTILE GUIDE

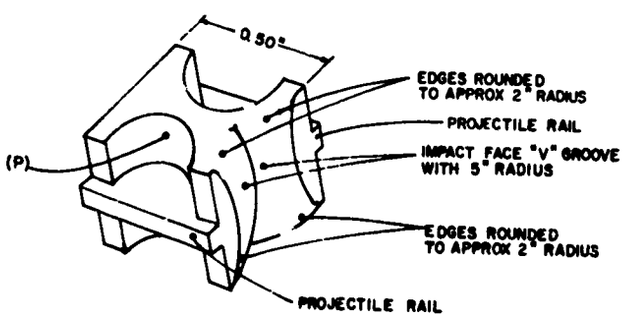

PROJECTILE

Figure 4. Slotted projectile guide and projectile

all experiments were constructed from aluminum and weighed approximately 5 grams. The semicylindrical sections (Figure 4) were machined from the body of the projectile to reduce projectile weight and also to provide a point on this projectile (P) which would lie in the same photographic plane as the test yarn and measurement scale.

The projectile is loaded into the slotted projectile guide from the front end. The test specimen is placed through the open slotted portion of the square barrel and the ends of the specimen are held by an upper and lower clamp. The test specimen is then aligned so that its long axis is perpendicular to the long axis of the barrel and aligned with the center of the impact face of the projectile. A gas reservoir is then pressurized, from a considerable larger volume tank of compressed helium, to the pressure required to obtain a desired projectile velocity. The pressure is released into the square slotted projectile guide by an electrically operated solenoid valve. Under conditions where the test specimen is completely broken the projectile goes into a catch box lined with soft felt. The same projectile can be used in a considerable number of experiments. The projectile velocity range extends from approximately 7 to 480 meter/sec for a projectile weight of 5 grams, and the gas pressure ranges from 10 to 1050 psi to obtain this velocity range. In order to obtain impact velocities above 330 meter/sec, without increasing the length of the square barrel portion of the projectile guide, a special membrane valve, designed by Lonnie M. Cole, was used. This valve is operated by presetting the desired reservoir pressure on one side of a 10-mil Mylar membrane and causing the membrane to rupture by very rapidly heating a nichrome wire formed in a single 0.6-inch-diameter open-ended loop clamped to the surface of the membrane. This valve provides for a 0.5-inch circular aperture from the reservoir straight through to the 0.5-inch square cross section of the slotted projectile guide.

b. High-Speed Photographic System. The arrangement and the components of the high-speed photographic system are shown in Figure 5. The operation of this system is as follows: A special holder permits positioning of a fine wire in the path of the projectile and is broken by the projectile before impact of the test specimen. The wire is positioned to one side of the test specimen impact area of the projectile. The wire is connected to an electronic pulser and the breaking of this wire triggers an Edgerton, Germeshausen and Grier, Inc. (EG&G) multiple microflash unit (Model 502) which then generates a sequence of ten light flashes equally spaced in time. Each flash is one microsecond in duration and the frequency of these flashes can be varied from 25 Hz to 100 KHz.

An Eastman commercial 8 x 10 inch still camera with a specially modified 10 x 12 inch Polaroid X-ray cassette is used. Just prior to the firing of the projectile the room is completely darkened and the camera shutter opened. When the projectile is fired, the light from the ten

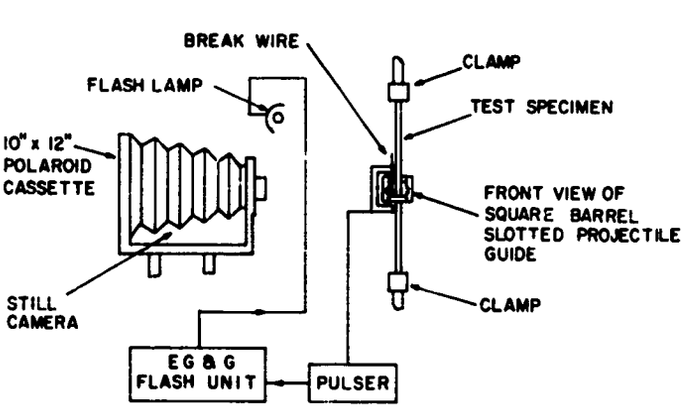

Figure 5. High speed photographic instrumentation

flashes is reflected from the successive positions of the test specimen and projectile thus producing ten separate images on a single 10 x 12 inch Polaroid radiographic packet type 3000X film. A Polaroid film processer manufactured by Picker X-Ray Company processes the film in ten seconds. Typical high-speed photographs of actual impacts are shown in Figures 6 and 8. The photographic field of view is 12 inches wide and the image magnification is approximately 0.8X.

3. Method of Holding Yarns

Several holding techniques were evaluated; however, only the technique used to acquire the data in this report will be discussed.

The clamps used are of the conventional-compression type tightened with a screw action and have 3/4-inch long by 1/2-inch wide smooth clamping faces. The yarn holding technique used in conjunction with these clamps involved the following procedure. Two smooth 1/8-inch diameter, 2-inch long steel pins are placed in slide fit holes drilled in a metal bar. The pin separation is equal to the distance from the top of the upper clamp to the bottom of the lower clamp and the yarn ends are tied on these pins with a knot. The pins with the yarn are then removed from the bar and the yarn is placed in the upper clamp with the steel pin sitting on the top of the clamp as seen in Figures 6 and 8. The clamp is tightened just enough to hold the yarn in place (small compressional clamping force). When more than one yarn is used, the bundle is given a 4-turn twist at

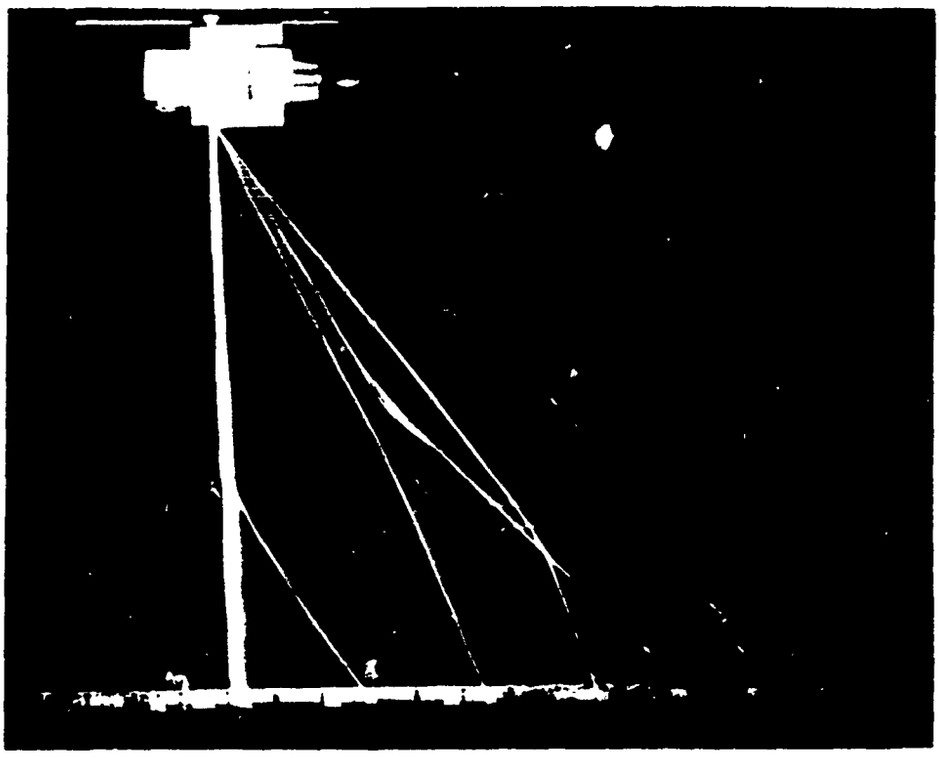

Figure 6. Photograph of yarn bundle impacted at low velocity, showing deformation and rupture. Bundle contains 4 yarns of Code C nylon 6/6 yarn. Impact velocity 104 meters per second. Time of 325 microseconds between flash exposures.

this time. The second pin together with the yarn is placed through the open slot portion of the projectile guide and positioned in the lower clamp in the same manner as in the upper clamp. When several yarns are used the bundle is formed with one continuous yarn looped around the two pins. The clamps are rigidly fixed to a table which provides x, y, and z orthogonal adjustment.

The edges of the clamping faces from which the transverse wave reflects were rounded with a 1/4-inch radius. Experimental results obtained when using clamp edges with a smooth right-angle geometry are very similar to those described below using a smooth right-angle projectile impact face.

Yarn breakage, when occurring at or near the clamped end, did not occur at the steel pins. The principal advantage of this holding method is that it provides for a fixed-end boundary condition which prevents yarn slippage and also eliminates high local compressive clamping stresses. The method relies on fiber-to-fiber friction and fiber-to-pin friction to provide the fixed-end condition. The method is presumably limited to somewhat nonbrittle fibers.

4. Effect of Yarn Pre-Tension and Twist

Specially designed experiments indicated that (1) variations of pre-tension on the yarn which were inherent in the experimental procedure, and (2) yarn bundles with no twist and a 4-turn twist, had no effect on the kinetic energy loss of the projectile within the sensitivity of measurements of the present testing instrumentation.

The reason for introducing a 4-turn twist when testing bundles of yarns was to provide conditions which make the bundle of yarns behave more as a single unit. This in turn provided better definition from the photographic record of (1) the position and time when complete breakage occurred, and (2) the transverse "tent like" displacement wave.

5. Measurement Procedures for the Determination of Projectile Kinetic Energy Loss

Projectile kinetic energy loss was calculated from projectile velocity measurements before impact and after complete breakage of the yarn test specimen. Draftsmen dividers were used to obtain the actual projectile travel distance from the photographic record of the impact with the aid of a photograph taken separately of a scale marked in millimeter divisions.

The times between successive flashes of the EG&G unit were used in the calculations of projectile velocities. The oscillator frequency of the EG&G unit which determines the time between flashes was measured with a 10-MHz Systron Donner counter timer.

6. Considerations of Instrumentation Parameters

a. Projectile-to-Guide Friction. One of the most important considerations involving the utilization of the slotted projectile guide concept is the determination of the loss in projectile kinetic energy resulting from projectile-to-guide friction. Experiments designed to evaluate this parameter have shown

that the frictional energy contribution is within the experimental data spread. These evaluation tests were conducted over a range of impact velocities extending from 60 to 340 meter/sec for the highest tenacity yarn only (Code A).

The first group of experiments involved the measurements of the uniformity of projectile velocity over the 12-inch slotted portion of the projectile guide with no test yarn. The projectile velocity measurements varied randomly within 2.5 percent over this 12-inch length.

The second group of experiments involved the measurements of projectile kinetic energy loss when the yarn is impacted in free flight. Free flight results showed good agreement with the related constrained projectile experiments. Free flight types of experiments are, in general, difficult to conduct and often limit the range of impact projectile kinetic energies which can be used with a particular yarn strength. These limitations are caused by projectile turning effects and departure of the yarn and projectile from the photographic film plane. Thus one of the advantages of the use of the GPT impacter is apparent here.

b. Projectile Impact Face Geometry. To minimize the effect of high local stresses introduced into the yarn by sharp or small edge radii of the projectile, the projectile's impact face was machined to have a 0.5-inch-radius 'V' groove with the upper and lower edges of the groove rounded approximately to a 0.2-inch radius. The purpose of the 'V' groove is to insure that the test yarn maintains its alignment with the center of the projectile during the time of impact and deformation.

Preliminary experiments employing a 'V' groove with smooth right angle edges have shown a considerable reduction in kinetic energy loss by the projectile, and a yarn breakage occurring at the impact face at considerably lower velocities than observed with the rounded impact face described above.

Projectiles with an 0.15-inch radius on the edge of the 'V' groove were also used and showed no difference from the 0.20-inch radius in the projectile kinetic energy loss. The projectile impact velocities ranged from 150 to 335 meter/sec for each of these impact face geometries.

B. Wave Propagation

Figure 6 is an actual photograph of a yarn bundle impacted at a low velocity, showing the progressive deformation of the specimen followed by the rupture. Also evident are the successive positions of the transverse wave, conforming closely to the behavior described by Smith et al.[6] According to Smith, the various yarn configurations can be depicted as in Figure 7. Position A shows the transverse wave propagating toward the clamps. Position B shows the transverse wave just at the clamps. Position C shows the reflected transverse wave propagating back toward the missile. Position D shows the transverse wave propagating toward the clamps after reflection at the missile. This behavior will continue until the yarn breaks. At low impact velocities we observed as many as four reflections before rupture.

In addition to the transverse wave, the impact produces a longitudinal wave which travels at the sonic velocity of the material. This wave is not visible in

our photographs and can be observed[4,9] only with difficulty, such as by marking the yarn at intervals and performing precise measurements on the photograph to detect displacement of the markings. The longitudinal wave velocity is generally greater than the transverse wave velocity;[9] hence, at a given time, its wave front is usually far ahead of the kink in the yarn which corresponds to the position of the transverse wave. Yarn rupture occurs either at the missile or at the clamp because the stress associated with the longitudinal wave increases at each reflection from a fixed boundary.

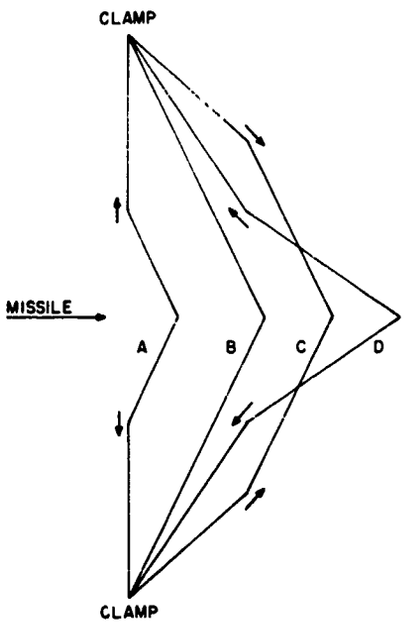

Figure 7. Various yarn configurations after transverse impact. Transverse wave reflects back and forth between missile and clamps as shown by arrows.

At higher impact velocities the yarn breaks sooner. If the impact velocity is sufficiently great, the yarn will break before the transverse wave reaches the clamp for the first reflection as shown in Figure 8. This is due to the high-stress level associated with the longitudinal wave, which means that fewer reflections of the longitudinal wave are required to produce yarn rupture. Thus the yarn breaks sooner and, if soon enough, the transverse wave will not have reached the clamp.

As an illustration of comparative wave velocities for a high-tenacity nylon yarn believed to be similar to the high-tenacity nylon yarn used by us, Smith et al.[9] observed a longitudinal wave-front velocity of 2800 meter/sec, whereas they found[8] transverse wave velocities ranging from 100 to 650 meter/sec for transverse impacts ranging from 0 to 650 meter/sec. Hence, in our experiments as exemplified in Figures 6 and 8, the longitudinal wave has reflected back and forth many more times than has the transverse wave.

C. Missile Kinetic Energy Loss

Each impacted specimen consisted of a number of parallel yarns twisted into a bundle. To determine the relative behavior of the four types of nylon yarn, it was desired to keep the weight per unit length approximately the same (10,000 denier) for the test specimens of all four yarns. Since the yarn deniers differed greatly, it was necessary to use different numbers of yarns per test bundle to give approximately this same bundle denier for all test specimens. The number of yarns used per bundle is shown in the accompanying table. Each test specimen was 12 inches in length.

Yarn Code	No. of Yarns Used per Bundle for Most Tests	Calculated Bundle Denier
A	12	10,356
B	140	9,926
C - Texturized	4	10,740
D - Undrawn	10	10,310

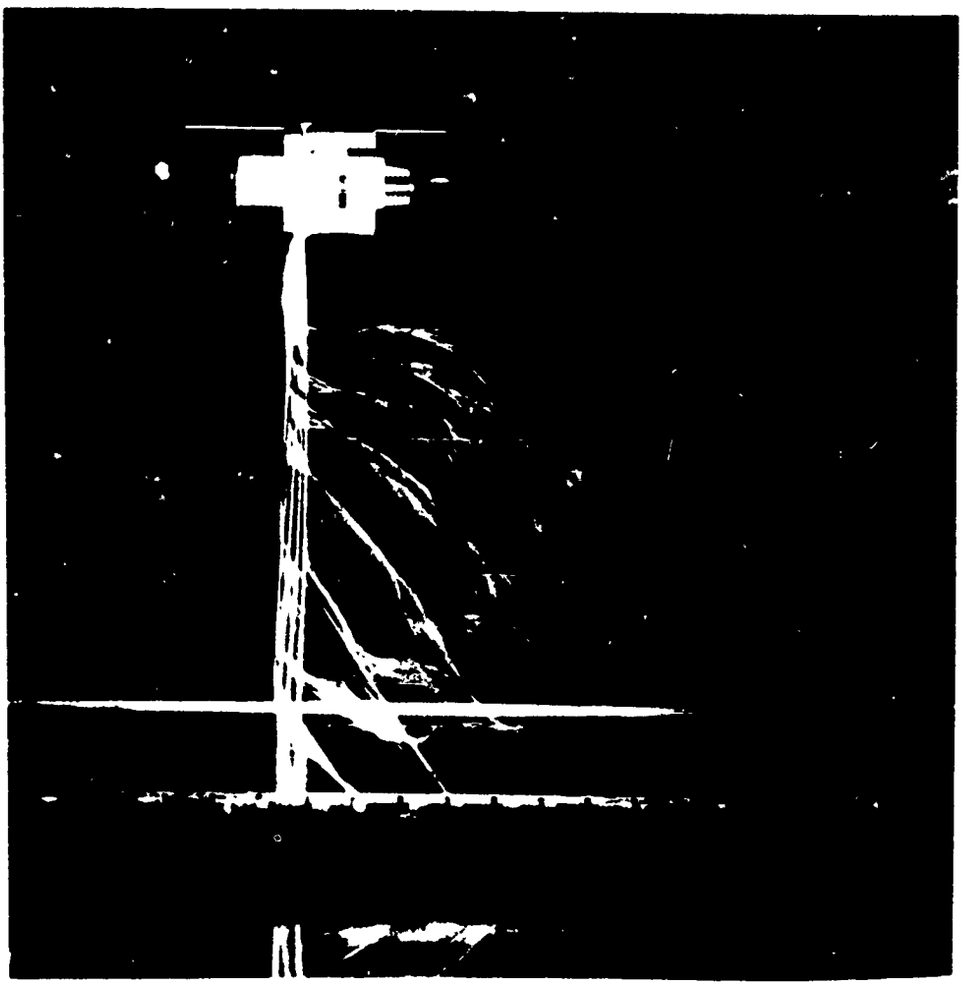

Figure 8. Photograph of yarn bundle impacted at high velocity showing deformation and rupture. Bundle contains 140 yarns of Code B nylon 6/6 yarn. Impact velocity 344 meters per second. Time of 75 microseconds between flash exposures.

To compare our energy data with values reported in the literature, we have followed the convention of expressing the results in terms of the energy divided by the mass of the yarn bundle, to give a normalized energy term in units of joules per gram of yarn.

Each of the data points reported below is the average of a number of shots, generally four. The averaged impact velocities and losses in missile kinetic energy for the yarns are presented in Table VI. To show the spread in energy, the maximum and minimum values are listed for each average impact velocity. It is seen that the energy spread is greater at impact velocities above those of peak energy loss. To illustrate the magnitudes of missile velocity decrements occurring during the tests, values of the initial and final missile velocities are presented for the cases of maximum and minimum energy loss. The average impact velocities and missile energy losses are also plotted in Figure 9. The general shapes of the curves are quite similar to each other, the main differences being the relative heights of the curves, their maximum values, and the velocities

Table VI. SUMMARY OF MISSILE IMPACT DATA OF FOUR COMMERCIAL NYLON 6/6 YARNS

Number Yarns/ Bundle	Impact Velocity, Avg m/sec	Energy Lost, Avg joule/g	Maximum Energy Lost			Minimum Energy Lost		
			Energy Lost, joule/g	Initial Velocity, m/sec	Final Velocity, m/sec	Energy Lost, joule/g	Initial Velocity, m/sec	Final Velocity, m/sec
Code A Yarn, Tenacity of 8.45 g/den								
1	26	48.2	51.6	26.5	7.9	45.7	25.9	10.3
1	60	55.7	61.0	58.8	52.0	46.3	62.0	57.2
1	92	52.2	72.9	92.5	87.5	33.3	92.5	90.2
4	93	54.6	55.9	93.0	76.7	53.5	93.0	77.5
12	92	51.5	56.3	90.5	10.7	49.7	92.7	35.0
4	100	63.7	71.4	100.8	82.7	58.8	98.5	83.4
12	135	64.6	66.4	133.5	92.3	63.5	134.6	96.1
12	169	80.1	81.6	171.0	131.5	77.1	167.5	129.5
12	170	70.6	73.6	168.7	134.8	66.5	170.0	140.0
12	234	87.3	89.8	233.3	204.7	83.9	233.3	206.6
12	267	124.4	144.2	272.0	232.0	110.5	263.2	232.2
12	298	131.9	138.7	300.8	266.6	122.6	293.3	262.5
12	316	152.1	167.1	319.0	280.0	139.9	313.0	280.0
12	321	138.0	145.7	322.2	288.9	135.5	320.0	289.0
12	333	156.4	169.2	337	298	137.7	331	299
12	336	134.8	149.4	340.0	305.9	111.5	330.6	304.7
12	338	138.4	160.3	341.2	305.9	120.2	337.6	311.7
12	354	118.8	140.7	358.6	330.0	89.7	347.1	328.5
12	372	82.0	123.2	373	348	28.6	372	360
12	395	101.8	144.7	400.0	378.5	76.6	393.8	380.0
12	417	0	0	424	424	0	409	409
Code B Yarn, Tenacity of 5.05 g/den								
10	29	39.2	40.1	29.9	21.7	38.1	27.1	18.3
70	62	35.3	36.1	62.4	35.0	34.8	61.7	35.1
140	107	35.7	42.4	108.3	73.8	29.2	105.2	82.2
140	153	41.6	41.9	152.0	130.0	41.4	156.5	135.5
140	192	50.9	53.8	193.6	172.6	48.0	190.8	172.0
140	224	54.6	58.5	226.4	206.4	49.5	221.4	204.3
140	276	88.1	96.5	275.0	248.7	83.7	276.2	253.7
140	305	71.4	92.3	315.0	292.5	40.5	305.0	295.0
140	333	47.0	53.1	333.3	321.3	41.3	332.0	322.7
140	345	21.5	30.9	346.7	340.0	12.3	344.0	341.3
140	377	0	0	377.3	377.3	--	--	--
Code C (Texturized) Yarn, Tenacity of 2.69 g/den								
<1	30	45.5	47.8	29.7	18.4	41.7	30.6	25.0
1	50	50.2	54.4	51.0	20.0	48.3	52.2	27.8
2	65	45.6	49.0	63.8	10.4	43.0	64.3	25.6
4	104	45.5	47.3	104.0	56.3	43.8	104.3	61.5
4	157	42.6	49.3	154.0	127.0	37.3	157.0	137.5
4	219	61.0	63.3	220.0	195.3	56.4	219.4	197.5
4	248	53.0	65.4	248.5	226.2	43.3	246.9	232.3
4	271	36.8	77.3	270.8	246.7	8.3	269.2	266.7
4	320	0	0	320	320	--	--	--
Code D (Undrawn) Yarn, Tenacity of 1.00 g/den								
10	66	12.2	13.3	64.9	46.7	11.0	67.0	53.0
10	103	14.9	15.1	104.3	92.6	14.2	103.1	92.0
10	135	20.3	20.4	135.3	123.3	20.3	134.7	122.7
10	161	21.4	22.6	162.0	151.0	20.3	159.5	149.5
10	186	9.6	11.0	185.7	181.1	8.3	185.7	182.3
10	200	0	0	200	200	--	--	--

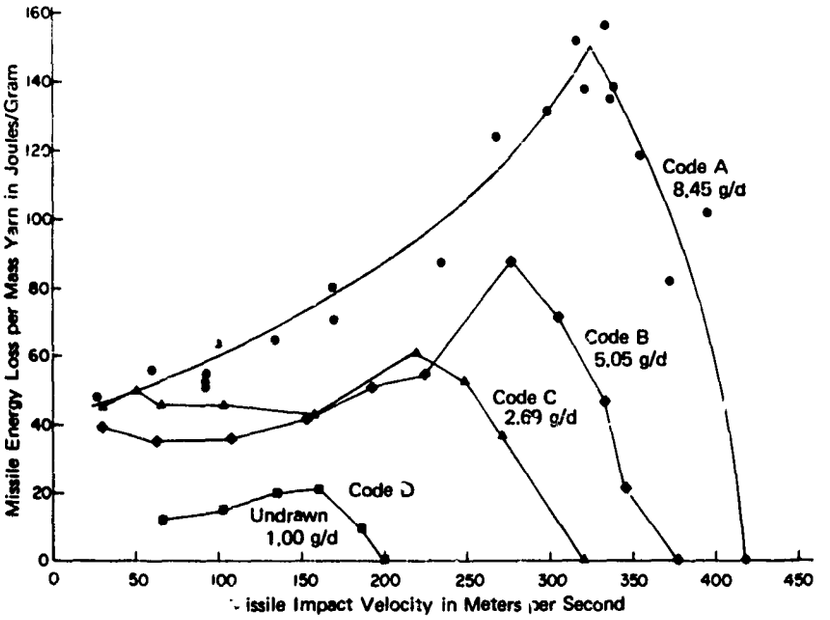

Figure 9. Missile energy loss (average) as a funtion of missile impact velocity (average) for the four nylon 6/6 yarns

at which occur the maximum values and zero values of the energy lost. It is seen from Figure 9 that, except for the two middle curves at velocities below 230 meter/sec, the heights and positions of the curves change monotonically with yarn tenacity (static). No special efforts were made to determine precisely the values or positions of these characteristic points of the curves, except for the highest tenacity yarn where enough data were taken to permit an average curve to be drawn rather than a point-to-point curve as with the other three yarns.

Here the comment should be made that, according to the manufacturer, their Code C yarn (tenacity of 2.69 g/den) has been subjected to a texturizing treatment which affects the tenacity. Obvious differences in this yarn are its greater denier and an appearance of being crimped. Hence, we are somewhat uncertain about the "true" or "effective" tenacity of this yarn. This difference in Code C yarn may be responsible for the inversion in position of this yarn and Code B yarn in Figure 9 at velocities below 230 meter/sec.

A few additional tests were run to determine the behavior of untwisted yarn bundles. These were performed with Code A yarn at impact velocities of about 170 and 340 meter/sec. The losses in missile kinetic energy did not differ significantly from those obtained at the same velocities with the standard 4-twist bundle. Hence, it was concluded that this twist (given to the yarn bundle for clearer images in the photographs) did not significantly alter the energy relationships being investigated.

Other tests were performed to determine the effect of bundle size upon the normalized energy loss of the missile. Some data for Code A yarn appear in Table VI where 1, 4, and 12 yarns per bundle were impacted at 92 to 93 meter/sec. It is seen that the energy loss ranged from 51.5 to 54.6 joule/g, showing

essentially no change. Some additional tests, not listed here, were done for this yarn with 24 yarns per bundle at impact velocities of 330 and 380 meter/sec. Again, the normalized missile energy losses did not differ significantly from those at these velocities with the usual 12 yarns per bundle. Hence, it can be concluded that within the scope of these bundle size variations at these impact velocities, the normalized missile energy loss is independent of the number of yarns per bundle.

The peak energy losses appearing in Figure 9 are plotted against yarn tenacity in Figure 10, along with longitudinal static breaking energies for the same yarns as reported in Section IIB of this report, Table IV. Figure 11 is a plot of two characteristic velocities obtained from Figure 9, again showing monotonic dependence upon yarn tenacity. Since the curves in Figure 10 could not be drawn smoothly through all the points, preference was given to the points representing the three yarns not subjected to the texturizing treatment.

In Figure 10 the monotonic increase of loss in missile energy with yarn tenacity is unmistakable. However, this is in contrast to the opposite dependence of the breaking energy during "static" Instron tests shown in Table I and Figure 10, indicating that certain of the energy absorption mechanisms must be significantly rate dependent. Further discussion of this will appear later in the report.

Referral again to Figure 9 shows the notable increase in missile kinetic energy loss with increasing impact velocity (at velocities below those of peak energy loss). It is obvious that the available kinetic energy of the missile increases with the square of the impact velocity. This increase in available missile kinetic energy with impact velocity is more rapid than the increase in the loss of missile energy during impact as is seen in the curves of Figure 12. Here the ratio of energy lost to energy available is plotted against missile impact velocity for each of the 3-bundle sizes for one of the yarn types. It is evident that the fraction of incident energy lost decreases as the impact velocity increases. Also apparent here is the reason for using several bundle sizes. The 12-yarn bundle at velocities below 92 meter/sec was causing a loss of nearly all the available kinetic energy. When the bundle size was reduced to 4 and then to 1 yarn, the fractional energy lost decreased correspondingly, giving a constant value for the normalized energy loss at this impact velocity, as discussed previously. On the other hand, the 1-yarn bundle could not be used at velocities above 92 meter/sec because only a

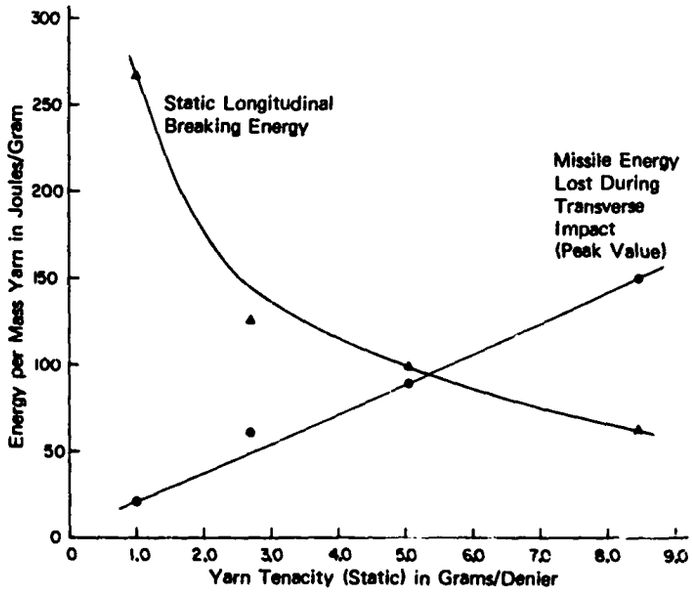

Figure 10. Peak missile energy loss and static breaking energy as functions of yarn tenacity for the four nylon 6/6 yarns

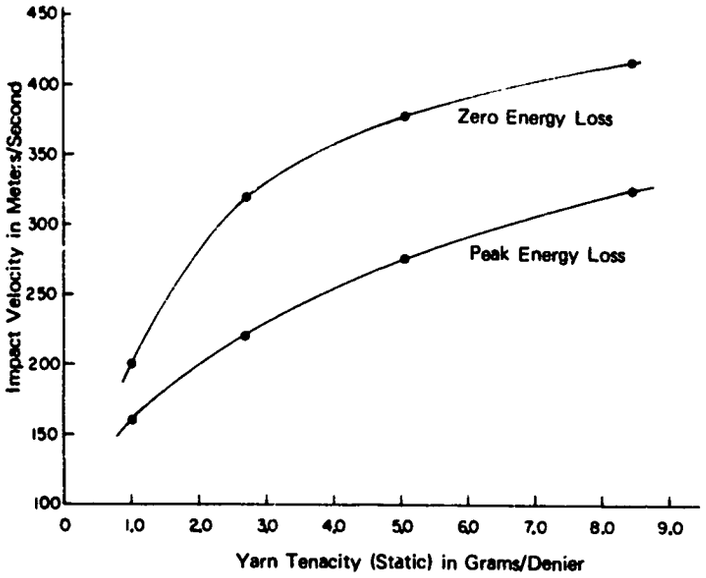

Figure 11. Impact velocity versus yarn tenacity for the four nylon 6/6 yarns. Lower curve: Impact velocity at which the missile energy loss reached the peak value. Upper curve: Approximate impact velocity at which the missile energy loss became zero.

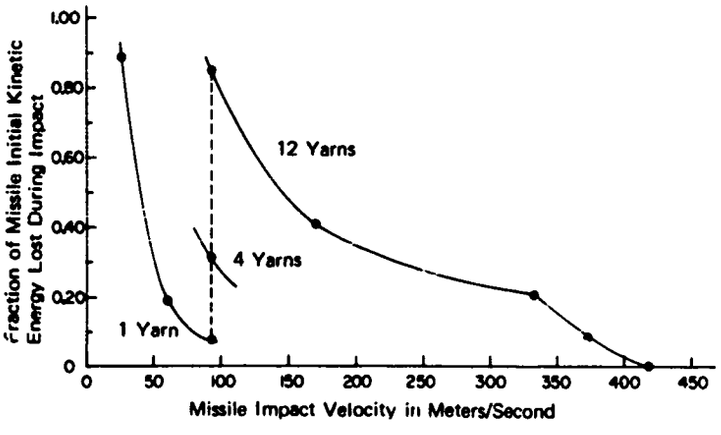

Figure 12. Fraction of initial kinetic energy of the missile lost during interaction with the yarn bundle as a function of missile impact velocity. Code A nylon 6/6 yarn.

negligibly small fraction of the incident kinetic energy was b ig lost. Hence, the impact v ocities at which the size of one yarn bundle is changed must be determined empirically and are chosen to maintain a ratio of energy lost to energy available which will not lead to inordinate errors in the determination of the energy lost.

It is also evident from Figure 12 that there appears to be a cusp in the curve at about 330 meter/sec, the velocity of maximum energy loss for this yarn as seen in Figure 9. This cusp is due to the beginning of the decrease in energy loss as a function of impact velocity and, hence, the ratio of energy lost to energy available will begin to decrease more rapidly at this point in Figure 12.

D. Other Experimental Observations

Measurements have been made from selected photographs regarding some of the details of the transient yarn deformation magnitudes. For example, with the highest tenacity yarn (Code A) the distance traveled by the yarn apex at the time of rupture is plotted against the missile impact velocity in Figure 13. Because the rupture occurs at a time which is unrelated to the time of the flash exposures, the rupture event can only be bracketed between two of the sequential flashes, namely, the last flash before rupture and the first flash after rupture. The data in Figure 13 are thus presented in this fashion, the actual distances falling somewhere between the two curves shown here. The data suggest

that the apex travel distance is fairly independent of impact velocity up to about 330 meter/sec, the velocity of maximum missile energy loss. At higher velocities the rupture occurs at much smaller travel distances. Hence, it appears that the average elongation-to-break decreases abruptly at the velocity of peak energy loss.

Estimates were then made by direct measurement of the percent average strain at break for the yarns during these transverse impact tests. Measurements were made of the yarn length in the last photo before rupture and in the first photo after rupture. (After rupture, this measured value would include whatever gap had appeared between the broken end and the clamp or the broken end and the missile, thus this value would be a maximum estimate.) These measured yarn lengths were then compared with the original yarn length to obtain the strain in the yarn just before and after break. Hence, the true strain value at break will be located somewhere between these two estimates. It was assumed that there was uniform strain in the yarn; hence, these estimated values are average values over the length of the yarn. These bracketing strain estimates appear in Figure 14 as a function of impact velocity for the highest tenacity nylon yarn (Code A). Several separate photographs were measured at each nominal impact velocity. The points plotted here are the highest strain value before break and the lowest strain value after break for each nominal impact velocity to reduce the size of this gap as much as possible. (Because the values for each pair of plotted points usually come from different experiments, the pairs of points are sometimes slightly displaced from each other on the velocity scale in Figure 14.) The method of presentation produces an irregular envelope within which the average breaking strains are located. From this plot and similar ones for the other yarns, it was concluded that the average breaking strains for each yarn were reasonably constant up to the velocity of peak energy loss of the missile and then decreased somewhat at higher impact velocities. This is shown by the dashed line in Figure 14. These average breaking strains are given in Table VII for the four yarns, along with the values obtained for the static longitudinal tests. It is remarkable

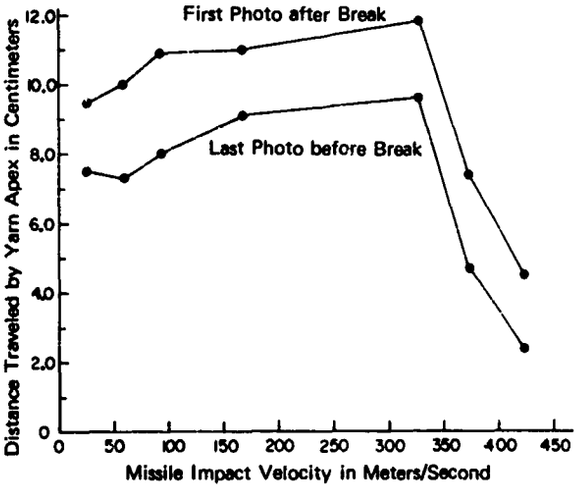

Figure 13. Distance traveled by yarn apex just before break and just after break as functions of missile impact velocity. Code A nylon 6/6 yarn.

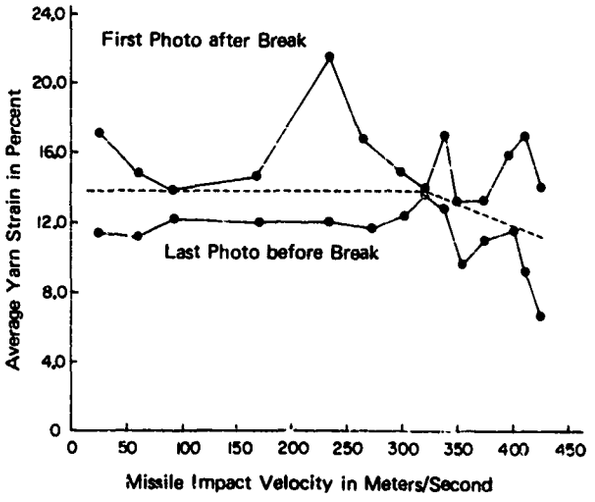

Figure 14. Average strain in yarn just before break and just after break as functions of missile impact velocity. Code A nylon 6/6 yarn.

that, except for the texturized yarn, the average dynamic breaking strains are about the same for all the yarns. The large differences between yarns observed statically are completely gone, producing a uniformly low value. The larger dynamic strain value for the texturized yarn indicates that even under the short times available during the impact test, there are some deformation modes accessible to this yarn and not to the others. However, the loss in missile energy for this yarn is not unduly great in relation to the other yarns as seen in Figure 10. Hence, this additional strain occurs without much additional energy absorption, thus suggesting that it may be largely a straightening of the crimp which involves very little energy.

Table VII. COMPARISON OF PERCENT BREAKING STRAINS

Yarn Code	Yarn Tenacity, g/den	Type of Test	
		Static Longitudinal, AMMRC	Avg. Impact, up to Velocity of Peak Energy Loss
A	8.45	17.3	13-14
B	5.05	30	12-13
C - Texturized	2.69	76	32-37
D - Undrawn	1.00	505	13-14

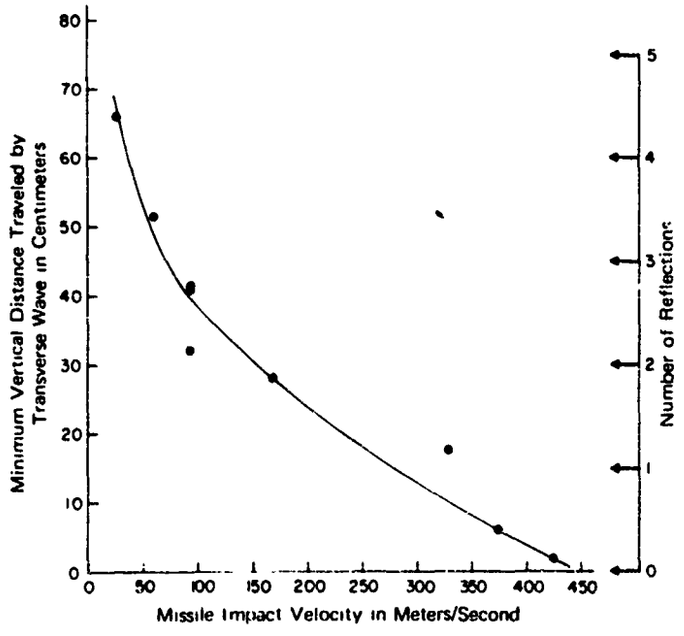

Figure 15. Minimum of the vertical component of the distance traveled by the transverse wave as a function of missile impact velocity. Code A nylon 6/6 yarn

With the same series of photographs for this yarn, measurements have also been made of the vertical component of the distance traveled by the transverse wave before rupture of the yarn. Again, this event can only be bracketed by the series of flash exposures, hence an exact determination is not possible. Because the position of the transverse wave tends to become indistinct after yarn rupture, it was possible to measure the transverse wave position only before rupture, thus giving the minimum of the vertical component of the distance traveled by this wave. This minimum distance is plotted against missile impact velocity in Figure 15. Although there is some scatter in the data, there is a definite decrease in wave travel distance with increasing impact velocity. The right-hand side of this graph indicates the approximate vertical travel distance corresponding to each reflection of the wave. Thus at the lowest velocity of impact there were four reflections before rupture, while at the highest velocities (above the velocity of peak energy loss of the missile) there were no reflections before rupture. An interesting application of this relationship may result from extrapolation of this curve to zero wave travel distance to give an estimate of the critical impact velocity. This will be discussed in more detail in the next section.

IV. DISCUSSION

A. Explanation of Curve Shapes

The explanation for the shapes of the curves in Figure 9 can be given in the following way.[11] The energy lost by the missile is acquired by the yarn bundle in the form of both strain energy and kinetic energy.

The maximum amount of storable strain energy is equal to the area under the appropriate dynamic stress-strain curve taken up to the dynamic breaking strain for the yarn. For our highest tenacity yarn (Code A), we assumed the stress-strain properties to be similar to those reported by Smith et al. for high-tenacity nylon.[8] From Figure 16 of that reference, we obtained an average dynamic modulus of 80 g/den. From our own work (Table VII), we took the dynamic breaking strain to be 14 percent. From the expression

$$\text{Breaking strain energy} = 1/2\ E\varepsilon_b^2 \qquad (2)$$

where E is the modulus and ε_b is the breaking strain, we calculated a breaking strain energy of about 70 joule/g of yarn. This is approximately the maximum strain energy that can be stored in this yarn under these conditions of high-speed loading.

For a given impact velocity, the yarn possesses the maximum amount of kinetic energy when the transverse wave has just reached the clamp to begin the first reflection. At this time the entire yarn specimen is undergoing transverse motion at the impact velocity (neglecting the slow down of the missile). For our highest tenacity yarn (Code A), the impact velocity causing peak energy loss (rupture occurs when the transverse wave reaches the clamps) was about 325 meter/sec. A simple calculation yields a value of yarn kinetic energy of about 50 joule/g for this impact velocity. A more detailed calculation, to include the effect of interaction of the reflected longitudinal wave with the transverse wave, gives a more accurate value of about 70 joule/g. This is then the maximum amount of kinetic energy this yarn can contain when subjected to the geometry and constraints of these impact tests.

Each curve appearing in Figure 9 comprises the sum of certain fractions of these maximum energy contributions. These can be discussed in terms of three regions of behavior.[11]

1. Quasi-Static Yarn Response

At very low impact velocities the kinetic energy term is very small for two reasons: (a) the low velocity term in the expression for kinetic energy, and (b) rupture does not occur until after a number of reflections of the transverse wave. By this time the entire yarn is no longer moving at the missile velocity; instead the transverse velocity distribution along the yarn ranges from zero at the clamped end to the missile velocity at the impact point, thus giving an average yarn transverse velocity considerably less than the missile velocity. For example, at a missile velocity of 30 meter/sec this average kinetic energy of the yarn is about 1/3 joule/g. Thus for tests conducted at these low missile

velocities, the kinetic energy term should vanish and each curve of Figure 9 should approach asymptotically the breaking strain energy for that yarn. This principle was used to furnish directly the breaking strain energy values at impact velocities of 25 to 30 meter/sec appearing in Figure 17.

2. Dyanmic *Yarn* Response

At very high impact velocities, the immediate strain produced at the point of impact exceeds the breaking strain and the yarn will rupture in a short time. The term "critical velocity" is often employed when dealing with quick rupture events and is considered to be the minimum impact velocity at which the breaking strain is immediately exceeded. However, because of time-dependent effects, the yarn does not break immediately but at a short time later, depending on the impact velocity as shown in Figure 11 of Reference 8. Hence, it becomes very difficult to determine experimentally the precise value of critical velocity. As the critical impact velocity is approached, the amount of energy absorbed by the yarn becomes very small because of the almost immediate yarn rupture. This reduces the amount of yarn involved in both the longitudinal strain energy term and in the transverse kinetic energy term. Hence, at progressively higher impact velocities the energy lost by the missile becomes smaller and smaller and tends to approach zero as seen in the curves of Figure 9. A useful working definition of the critical velocity might be the minimum impact velocity at which (a) the missile energy loss becomes zero (as seen in Figure 9), or (b) the transverse wave travel distance becomes zero (by extrapolation of Figure 15).

3. Dynamic *System* Response

At intermediate impact velocities, the loss in missile energy increases to a peak and then decreases. As the impact velocity is increased from the lower values, the kinetic energy content of the yarn in transverse motion increases with the square of the velocity, causing the observed rise in the missile energy loss. At the same time, the number of reflections of the transverse wave (prior to rupture) decreases with increasing impact velocity as shown in Figure 15. The peak energy loss occurs at the impact velocity at which the yarn breaks just as the transverse wave reaches the clamp for the first time, because under this condition the entire yarn specimen is moving at the missile velocity, and thus, at this point, the kinetic energy component of the yarn is at a maximum. At higher impact velocities the yarn breaks before the transverse wave reaches the clamp. This decrease in the amount of yarn involved in the transverse wave motion more than compensates for the increased velocity and thus the kinetic energy content of the yarn decreases. As the critical velocity is approached, the amount of yarn involved in the longitudinal strain energy region also decreases and hence both energy components of the yarn decrease toward zero.

It is interesting to note that for the highest tenacity yarn (Code A), the estimates made at the beginning of this section for the maximum strain energy component and kinetic energy component were both 70 joule/g, giving a total estimate for the peak of this curve as 140 joule/g. This estimate is in reasonable agreement with the experimentally determined average of about 150 joule/g appearing in Figure 9. Unfortunately, this kind of comparison cannot be discussed for other portions of the curves, because theoretical estimates of the kinetic energy and strain energy components cannot be readily made for these other velocity regions since the appropriate dynamic moduli values are not known.

From the preceding analysis, it becomes apparent that at a given impact velocity the kinetic energy component for all four yarns (below the velocity of peak energy loss) is essentially the same, neglecting any differences in the longitudinal particle velocity term. This is because the yarn masses per unit length are all the same (about 10,000 denier) as are the transverse yarn velocities. Therefore, at a given impact velocity the differences in energy loss from yarn to yarn are due only to differences in the strain energy components. If the strain energy to break is constant for each yarn, the curves in Figure 9 should all rise equally with impact velocity, maintaining constant differences between them. Or, if the strain energy to break for all four yarns has the same rate dependence, the curves should also rise equally and maintain the same differences. Examination of Figure 9 indicates that there is some nonuniformity in the curves, i.e., they rise at somewhat different rates. This implies that the breaking strain energies of the yarns have somewhat different strain rate dependences.

Even though it is now apparent that the data appearing in Figures 9, 10, and 11 include effects due to kinetic energy components as well as to strain energy components, the curves show the importance of yarn tenacity in determining the total energy loss of the missile. In particular, Figure 11 shows the role of tenacity or modulus in the impact performance of nylon yarns, for not only are the missile energy losses increased for high-tenacity yarns but also the velocity ranges over which can occur useful energy losses are correspondingly extended.

B. Apparent Similarity to Ballistic Data for Felts

The yarn behavior noted in Figure 9 is similar to that observed for textile materials in the form of felts which have been impacted with the standard 17-grain fragment simulator. From ballistic limit studies combined with residual velocity measurements, plots may be constructed showing the reduction of projectile kinetic energy as a function of impact velocity[12] as shown in Figure 16.

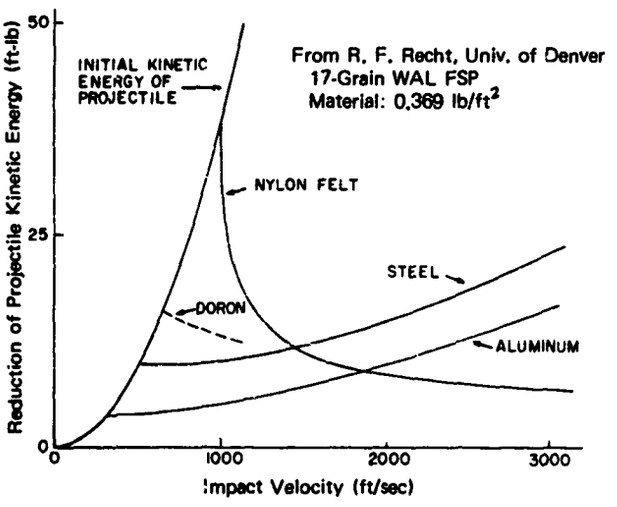

Figure 16. Ballistic results for four materials compared at the same areal density: reduction of projectile kinetic energy as a function of impact velocity.

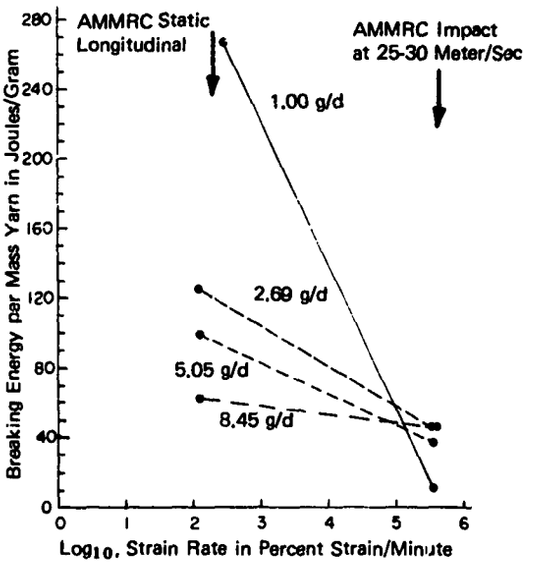

Figure 17. Breaking energy for the AMMRC static test and the AMMRC low-speed impact test as a function of log strain rate for each of the four nylon 6/6 yarns

Here the curve for the nylon felt follows the initial kinetic energy curve for the projectile up to the ballistic limit (V_{50} value) and then decreases rapidly toward zero although it levels off before actually reaching zero. This abrupt decrease in loss of missile kinetic energy above the ballistic limit does not occur for the steel, aluminum, and Doron in Figure 16, and thus appears to be peculiar to textile materials.

This similarity in shape of the energy loss curves for the yarns (Figure 9) and for the felts (Figure 16) suggests that high-speed impact tests with yarns may be useful indices of performance for textile materials in forms more related to end items, such as fabrics and felts. The implication here is that there may be some fairly direct relation between the ballistic limit velocity for the felt (expressed as the velocity of maximum energy absorption per unit areal density) and the velocity of peak missile energy loss for the yarn. In other words, for the felt subjected to a ballistic test, there may be a characteristic velocity at which the projectile kinetic energy absorbed per unit felt areal density reaches a maximum value, and this may be related in a potentially informative way to the velocity of peak energy loss as observed in these yarn impact studies.

C. Estimated Strain Rates of the Impact Tests

Virtually all of the data reported in the literature concerning dynamic behavior of textile yarns are expressed in terms of the strain rate where machine-type testing is involved. To make comparisons with our impact results to examine the rate dependences, we must be able to express our impact testing in terms of an estimated strain rate. An analytical expression for the strain rate can only be an estimate because of a variety of complicating factors. Therefore, we have adapted the following simplifications: (1) the presence of the transverse wave is ignored and we consider that the yarn is always in the form of a smooth triangle defined by the apex and the two clamps; and (2) we assume that the entire yarn is strained to the same degree, i.e., there are no strain gradients. With these simplifications in mind, we consider Equation 1 developed in Section IIB for the static transverse tests.

$$\text{Strain rate} = \frac{x}{l_0\sqrt{l_0^2 + x^2}} \frac{dx}{dt} \tag{1}$$

where x is the apex travel distance, l_0 is one half the original specimen length, and dx/dt is the instantaneous missile velocity. For very large apex travel distances ($x >> l_0$), this equation reduces to

$$\text{Strain rate} = \frac{1}{l_0} \frac{dx}{dt} \tag{3}$$

With this simplified expression the strain rate is independent of x. This equation leads to the values presented in Table VIII. According to this approximation, our impact tests produced strain rates of the order of 10^6 to 10^7 percent strain per minute. However, these appear to be maximum estimates because (1) the yarns actually break before x greatly exceeds l_0, thus the actual strain rates are lower; and (2) the missile velocity (dx/dt) becomes smaller during the course of the test, thus also decreasing the strain rate.

A better estimate of the strain rate can be made by the use of Equation 1 if more accurate values of x and dx/dt are available. Since Equation 1 was derived on the basis of a smooth triangular shape of the yarn, Equation 1 would be valid only for times when the transverse wave had just reached the clamps. This condition obtains at the peak of the energy loss curves in Figure 9 because rupture occurs just when the transverse wave reaches the clamp. For example, with the highest tenacity yarn (Code A), the peak energy loss is 150 joule/g at an impact velocity of 325 meter/sec. Knowing the mass of the yarn specimen (0.350 g) and the mass of the missile (4.74 g), we calculate the corrected missile velocity (dx/dt) at the time of rupture to be 2.89×10^4 cm/sec. From our previous estimate of the breaking strain of this yarn as 14 percent, and knowing the value of l_0 (6 inches) to be 15.24 cm, we obtain a value of missile travel distance (x) at the time of rupture of 8.35 cm. Putting these values of x, l_0, and dx/dt into Equation 1, we calculate the value of strain rate at the time of rupture to be about 5.5×10^6 percent strain/min. This value is about 43 percent of the value estimated by Equation 3 in Table VIII at the same impact velocity of 325 meter/sec. Thus, by the use of a corrected (smaller) value of dx/dt (289 instead of 325 meter/sec) and by using a real value of x (instead of simply letting $x >> l_0$), we can obtain an estimate of the strain rate at the time of yarn rupture. However, this more accurate expression (Equation 1) can only be used under those conditions where the necessary data are sufficiently well known.

A more direct measure of the strain rate can be made from the type of photo measurements already described in Section IIID which led to estimates of the percent average strain at break. From measurements of the yarn length in the last two flash exposures before yarn rupture, the percent strain at these two times was determined (again with the assumption of uniform strain in the yarn). Knowing the time between these two flashes, one can immediately compute the percent average strain rate during this portion of the deformation. For impact velocities in the range of 25 to 30 meter/sec, the measured strain rates ranged from 3×10^5 to 4×10^5 percent strain/min. For impact velocities in the range of 325 to 355 meter/sec, the strain rates ranged from 3×10^6 to 6×10^6 percent strain/min. These results are listed in Table IX. Comparison of these values with those estimates appearing in Table VIII indicates that these measured values are 25 to 50 percent of the values estimated by Equation 3. This confirms the

Table VIII. ESTIMATED STRAIN RATE AS A FUNCTION OF MISSILE IMPACT VELOCITY (FROM EQ. 3)

Impact Velocity, dx/dt, meter/sec	Strain rate, % strain/min
25	0.98×10^6
100	3.94×10^6
225	8.86×10^6
325	1.28×10^7
425	1.67×10^7

Table IX. COMPARISON OF ESTIMATED STRAIN RATES FOR AMMRC LOW AND HIGH VELOCITY IMPACT TESTS

Impact Velocity, meter/sec	Estimated Strain Rate, % strain/min		
	By Eq. 3	By Eq. 1	By Photo Measurements
25	0.98×10^6	--	$3\text{-}4 \times 10^5$
325	1.28×10^7	5.5×10^6	$3\text{-}6 \times 10^6$

approximate nature of Equation 3 and its tendency to overestimate the strain rate. It is also seen that these measured strain rates for impact velocities in the 325 to 355 meter/sec region are in good agreement with the value of 5.5×10^6 percent strain/min calculated for this velocity region by the use of Equation 1.

What cannot be assessed, however, is the local strain and strain rate at the portion of the yarn where failure occurs. If the strain gradients are large, it is possible that the local strain rate in the failure region might be considerably different from these estimated values. Hence, our estimates are intended only as a rough guide for comparisons to published data.

D. Comparison of Yarn Breaking Energies With Fracture Energy Calculated From Molecular Parameters

It is of interest to compare the values of energy required to break the yarns in these impact tests to the values of fracture surface energy calculated with the aid of a simplified molecular model. The model assumes that the molecular chains are all perfectly aligned parallel to each other and perpendicular to the fracture surface. The breaking energy would then be that energy required to break one molecular bond for each chain passing through the plane of the fracture surface. The fracture surface area would be the yarn cross-sectional area and was computed to be 9.7×10^{-3} sq cm from the value of 10,000 denier and a volume density for nylon of 1.14 g/cu cm. The number of molecular chains crossing this area was computed as 4.7×10^{12} from the estimated value of 20.5 Å^2 for the cross-sectional area of a hydrocarbon chain.[13] The energy of a carbon-carbon single bond was taken to be 83.1 kcal/mole.[14] These figures yielded a value of 2.7×10^{-6} joules required to break a 10,000-denier nylon yarn along one plane perpendicular to the yarn axis.

The breaking energies for our yarns (exclusive of the kinetic energy components) were estimated to range from 10 to 70 joule/g. Since the yarn specimens have been approximately 10,000 denier and are 12 inches long (mass of 0.338 g), these breaking energies range from 3.4 to 24 joules. These give ratios of actual breaking energy to theoretical bond breaking energy ranging from $3.4/2.7 \times 10^{-6}$ to $24/2.7 \times 10^{-6}$ or 1.2×10^6 to 8.8×10^6. Therefore, there is of the order of 10^6 to 10^7 more breaking energy involved than that due simply to bond breakage at one plane, indicating that strain energy stored in the entire yarn length far exceeds that required to cause rupture at just one point in the yarn.

It is interesting to note that these ratios of 10^6 or 10^7 greatly exceed the value of about 10^3 for the ratio of measured to theoretical surface energy for Plexiglas, a rigid polymer in sheet form.[15] The much higher ratios for the yarn are apparently due to the fact that the yarn absorbs strain energy along its entire length; whereas for a sheet polymer, such as Plexiglas, the depth of the resultant oriented layer along the fracture surface may be only about 1500 Å.[15] Thus with the yarn, far more peripheral material is involved in the deformation process than with the sheet polymer.

E. Effects of Tenacity and Rate

1. Shape of Static Breaking Energy Curve as a Function of Tenacity

With the static tests there is a marked dependence of breaking energy upon tenacity as seen in Figures 2 and 10. The large amount of deformation and drawing which occurs during the test with the low-tenacity yarns apparently more than offsets the low tenacity of the yarns, thus resulting in a high value of breaking energy. The amount of deformation and drawing which can occur during the test becomes less with the higher tenacity yarns because these higher tenacities have been produced by prior cold drawing which presumably has "used up" more of the total available deformation. Hence, the static breaking energy becomes progressively lower with higher tenacity yarns.

2. Shape of Peak Missile Energy Loss Curve as a Function of Tenacity

In Figure 10 the peak missile energy loss increases with increasing yarn tenacity. We have already seen that the missile energy loss is divided between a kinetic energy term and a strain energy term. For the low-tenacity yarns, the peak energy losses plotted in Figure 10 were obtained at low-impact velocities as seen in Figure 9. Thus, the kinetic energy component is smaller for the low-tenacity yarns than for the high-tenacity yarns. Also we have seen that the impact breaking strains were essentially the same for all the yarns (except the texturized one). Since the breaking stresses would decrease with decreasing yarn tenacity or decreasing modulus, the strain energy component would be smaller for the low-tenacity yarns than for the high-tenacity yarns. Hence, both the kinetic energy and the strain energy components would change with yarn tenacity in such a way as to give the trend exhibited in Figure 10 for the total missile energy lost during impact.

3. Relative Energy Magnitudes for Low-Yarn Tenacities

At the low tenacity end of the curve of missile energy loss in Figure 10, the strain energy component is obviously much less than the longitudinal static breaking energy plotted above it. This lower value is undoubtedly due to a rate effect, where the time available is so small during the impact test that these large deformation and drawing processes cannot occur as seen by a comparison of breaking strains in Table VII. In other words, the energy absorbing mechanisms available to the low-tenacity yarns at low rate testing simply cannot be utilized at the rates corresponding to the impact tests.

4. Relative Energy Magnitudes for High-Yarn Tenacities

At the high tenacity end of Figure 10, the curve for the missile energy loss has higher values than that for the static longitudinal test. For the highest tenacity yarn (Code A), we have already seen that the breaking strain energy component for the impact test has been estimated at about 70 joule/g at an impact velocity of 325 meter/sec. This value is comparable to the value of breaking energy obtained for both the AMMRC static longitudinal and static transverse tests, and is only slightly less than the manufacturer's static longitudinal value. Therefore, apparently the characteristics of this yarn are such that the breaking stress at high rates is enough higher than that at low rates to

compensate for the decreased breaking strain shown in Table VII and can thus keep the strain energy component at a high value. (It must be remembered that the high tenacity end of the missile energy loss curve in Figure 10 also includes a large component of kinetic energy and hence the total energy plotted here exceeds by a large amount the energy shown plotted below it for the static test.)

5. Breaking Energy as a Function of Strain Rate

The breaking energy data obtained at AMMRC with the series of four nylon yarns are presented in Figure 17 for both static and low-speed impact tests. The static energies plotted here from Table IV are the longitudinal ones because of the uncertainties associated with the transverse static test. The low-speed impact (25 to 30 meter/sec) energies plotted here were taken from Figure 9 either directly or by extrapolation. These values can be considered the breaking strain energy because we have seen in Section IVA that at this low-impact velocity the kinetic energy component is negligible.[11] The strain rates corresponding to the static tests are those listed in Table II; the strain rate for the low-speed impact test is taken from the photo measurement method as listed in Table IX. In Figure 17 the breaking energy decreases with increasing strain rate for all four yarns. It is also evident that the rate of decrease with strain rate is greatest for the low-tenacity yarn and the rate decreases monotonically with increasing yarn tenacity. Thus, the yarns exhibit great differences in their rate dependence. The breaking strain data in Table VII also indicate large differences in the rate dependence as seen from the marked variations from yarn to yarn in breaking strain increment between the static value and the impact value.

F. Comparison to Published Results

Breaking energy data for nylon yarns, obtained by other investigators,[1,2,7] are plotted in Figure 18 as a function of strain rate. These other tests were all longitudinal in nature and were performed with testing machines except for one test done by transverse impact at 41 meter/sec. Most of these other tests show a decreasing breaking energy with increasing strain rate as do our tests shown in Figure 17.

The breaking energies obtained by us for the high-tenacity nylon (Code A) are also plotted in Figure 18 from the data given in Table X (the first two points for this yarn are also plotted in Figure 17). The static breaking energy listed in Table X was the longitudinal value rather than the transverse value because of the uncertainties associated with the latter test. The breaking energy for the

Table X. SUMMARY OF BREAKING ENERGIES AND STRAIN RATES

Breaking Energy, joule/g	Impact Velocity, meter/sec	Estimated Strain Rate, % strain/min	SOURCES OF DATA
62	--	1.2×10^2	AMMRC Static Longitudinal Test.
45	25	3.5×10^5 (average)	AMMRC Impact Test and Photo Measurements as given in Table IX.
70	325	5.5×10^6	AMMRC Impact Test, Reference 8, and Eq. 2 for the energy; Eq. 1 as given in Table IX for the strain rate.

25-meter/sec impact could be taken directly from the average curve for this yarn as shown in Figure 9 because at this low-impact velocity the kinetic energy component is negligible[11] as pointed out in Section IVA. The value listed for the 325-meter/sec impact was that energy estimated[11] by Equation 2 in Section IVA for a similar high-tenacity nylon yarn impacted transversely.[8]

An overall view of Figure 18 shows the general trend of decreasing breaking energy with increasing strain rate. The first two points for the yarn we studied (Code A) fit right in with this trend. The two nylons in Figure 18 showing the highest absolute values and the greatest negative slopes were those studied by Hall[2] (Enkalon and Nylon 100), and have relatively low tenacities (4.3 and 5.3 g/den, respectively) compared to the other yarns in this figure. Thus, these low-tenacity yarns exhibit the same relative behavior (high breaking energy and large rate dependence) as the low-tenacity yarn studied by us and shown in Figure 17. The yarn in Figure 18 with the highest values of breaking energy is the undrawn nylon 6/6[1] (tenacity less than 1 g/den), again agreeing with our data as shown in Figure 17. However, the opposite rate dependence of this yarn in Figure 18 is not understood, although this rate dependence may be equivalent to that of the high-tenacity nylon studied by Smith et al.[7] in Figure 18 at lower rates which also shows this opposite rate dependence.

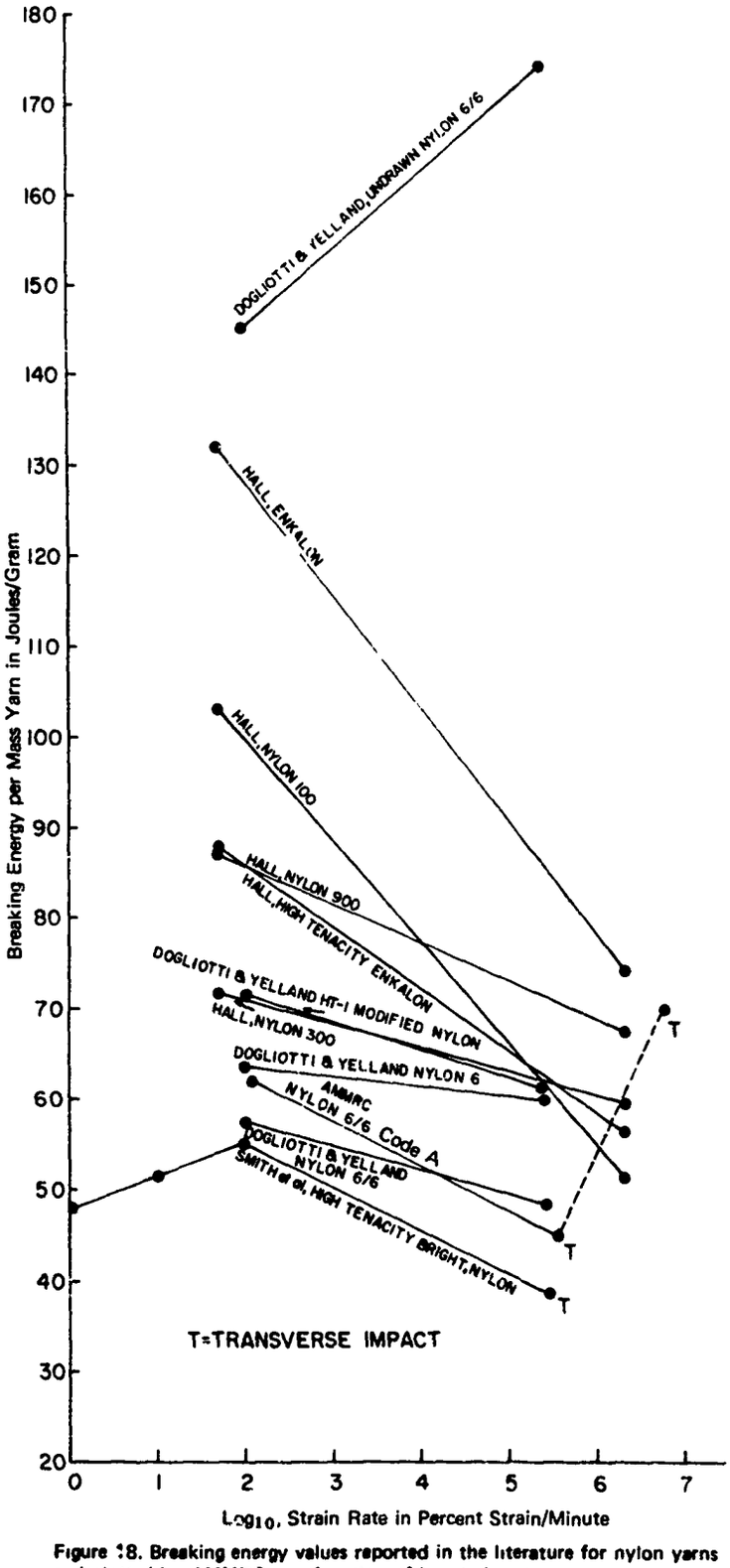

Figure 18. Breaking energy values reported in the literature for nylon yarns and plotted by AMMRC as a function of log strain rate

In other words, the low-tenacity nylon may show behavior similar to the high-tenacity nylon if it is studied at correspondingly higher strain rates.

Our impact tests have produced strain rates higher than those attainable by machine-type tests (5.5×10^6 compared to 2.0×10^6 percent strain/min). However, the value of missile kinetic energy loss determined by our method also includes the yarn kinetic energy component which is difficult to evaluate. Hence, the strain energy component which is needed for direct comparison with the data in Figure 18 is not directly available. We have seen that for a high-tenacity nylon yarn believed similar to the one we have studied (Code A), a combination of published data[7,8] and our own measurements has led to an estimated breaking energy of 70 joule/g at an impact velocity of 325 meter/sec. This estimate can be further substantiated by the calculation made for this report in Section IVA[11] of 70 joule/g for the yarn kinetic energy component at this impact velocity. Subtracting this latter value of 70 joule/g from the total missile energy lost (150 joule/g at this impact velocity as seen in Figure 9) gives a strain energy component of about 80 joule/g. This agrees fairly well with the direct estimate of 70 joule/g for the strain energy component. This value of 70 joule/g which appears in Table X was plotted as an additional point for the yarn studied by us (Code A) in Figure 18, thus indicating a reversal to an upward trend in the breaking strain energy as a function of strain rate. This result shows a significant change in what has previously been considered by us as a steadily decreasing breaking energy with increasing strain rate for nylon yarn.

Some support for this apparent minimum in the breaking energy curve as a function of strain rate comes from a closer look at the results of Smith et al.[8] In Figure 16 of that reference are plotted stress-strain curves for high-tenacity nylon yarn studied at various strain rates. The breaking energies corresponding to the curves at 1, 10, 100, and 290,000 percent strain/min are those tabulated in Reference 7 and plotted by us in Figure 18. This breaking energy decreases in the interval between 100 and 290,000 percent strain/min, in concert with the general trend displayed in Figure 18. Returning now to Figure 16 of Smith et al.,[8] one finds two more stress-strain curves plotted from $\bar{U}$, V data obtained at still higher impact velocities (495 and 650 meter/sec). By measuring the areas under these curves, it was found that the breaking energy continued to decrease to the value of 18 joule/g at 495 meter/sec impact velocity but then increased to a value of 35 joule/g at 650 meter/sec. Therefore, these results of Smith et al. also indicate a minimum in the breaking energy of nylon yarn followed by an increase at still higher strain rates.

Still more confirmation for this minimum in the breaking energy of nylon yarn is found in some recent work of Hall.[16] He determined the stress-strain curves for nylon 6/6 and other yarns at a series of strain rates ranging from 0.6 to 2×10^6 percent strain/min by the use of testing machines. The areas under the curves provided values of the breaking energies of these yarns. For the nylon 6/6 yarn, the breaking energy as a function of strain rate showed the same behavior as the data of Smith et al.[7] which we have plotted in Figure 18. The data of Hall[16] show a maximum (about 70 joule/g) at low strain rates, followed by a minimum (about 35 joule/g) at higher strain rates. The approximate strain rates of these maximum and minimum breaking energies are listed in Table XI along with that for the minimum found in our work at AMMRC. It is seen that where comparisons can be made there is a general agreement for these strain rate values, even though the data points of Smith et al.[7] and AMMRC are not numerous enough to locate precisely these critical strain rates.

Table XI. STRAIN RATES OF NYLON 6/6 YARNS AT MAXIMUM AND MINIMUM BREAKING ENERGIES

Investigator	Breaking Energy (joule/g)		Strain Rate (%/min)	
	Maximum	Minimum	at Maximum Energy	at Minimum Energy
Smith et al.[7,8]	55	(18)*	1.0×10^2	(495 m/sec)†
Hall[16]	70‡	35‡	1.5×10^2‡	9.0×10^4‡
AMMRC	--	45	--	3.5×10^5

*Estimated by AMMRC from Figure 16 of Reference 8
†Available only as impact velocity
‡Estimated by AMMRC from Figure 7 of Reference 16

V. CONCLUSIONS

The transverse impact method in combination with high-speed photographic observation has been shown to provide a wealth of information regarding the transient behavior of missile and yarn during the impact, deformation, and rupture processes. The determination of the missile kinetic energy loss provides a direct measure of the total energy absorbed by the yarn during these processes which occur at high rates. Other measurements provide information concerning the apex travel distance, breaking strain, transverse wave propagation effects, and an estimate of critical velocity. All of these phenomena can be studied as functions of impact velocity and as functions of systematic variations in yarn properties, such as tenacity, as described in this report. It is believed that this study has been one of the first to focus upon the transient behavior of a series of systematically related yarns subjected to high-speed transverse impact.

It is not known at the present time whether the strain energy component or the total energy lost by the missile or absorbed by the yarn is the quantity which can be most closely related to the ballistic performance of more complex structures, such as fabrics and felts, made from fibers and yarns of these same materials. It has already been pointed out that the resemblance between our total energy loss curves for yarns and those obtained from ballistic testing of nylon felts may be significant. However, where the interest lies in determining the strain energy component of the total energy absorbed by impacted textile yarns at high-strain rates, the method described by Smith et al.[8,9] would be preferred. From separate determinations of the breaking strain, the stress-strain curve could then yield the value of breaking strain energy.

The necessity of high-speed testing becomes apparent from a comparison of nylon and polypropylene; nylon fabric generally has a better ballistic performance than that of polypropylene, whereas comparison of their static breaking energies would lead to the opposite prediction.[17] Obviously, the laboratory tests must be conducted at rates comparable to those obtaining for actual ballistic events. Further investigations are necessary to develop useful predictive relationships between laboratory tests of the type described here and actual ballistic performance of end item structures composed of these textile elements.

LITERATURE CITED

1. DOGLIOTTI, E. C., and YELLAND, W. E. C. *Effect of Strain Rate on the Viscoelastic Properties of High Polymeric Fibrous Materials.* High-Speed Testing, v. IV, Interscience, New York, 1964, p. 211.

2. HALL, I. H. *The Tensile Properties of Textile Yarns at Very High Strain Rates.* High-Speed Testing, v. IV, Interscience, New York, 1964, p. 237.

3. PILSWORTH, M. N. Jr. *Tensile Impact on Rubber and Nylon.* Quartermaster Research and Engineering Center, Natick, Massachusetts, Technical Report PR-3, May 1962.

4. PETTERSON, D. R., STEWART, G. M., ODELL, F. A., and MAHEUX, R. C. *Dynamic Distribution of Strain in Textile Materials Under High-Speed Impact. Part I: Experimental Methods and Preliminary Results on Single Yarns.* Textile Res. J., v. 30, 1960, p. 411.

5. PETTERSON, D. R., and STEWART, G. M. *Part II: Stress-Strain Curves from Strain-Position Distributions.* Textile Res. J., v. 30, 1960, p. 422.

6. SMITH, J. C., McCRACKIN, F. L., SCHIEFER, H. F., STONE, W. K., and TOWNE, K. M. *Stress-Strain Relationships in Yarns Subjected to Rapid Impact Loading. Part IV: Transverse Impact Tests.* Textile Res. J., v. 26, 1956, p. 821.

7. SMITH, J. C., SHOUSE, P. J., BLANDFORD, J. M., and TOWNE, K. M. *Stress-Strain Relationships in Yarns Subjected to Rapid Impact Loading. Part VII: Stress-Strain Curves and Breaking-Energy Data for Textile Yarns.* Textile Res. J., v. 31, 1961, p. 721.

8. SMITH, J. C., FENSTERMAKER, C. A., and SHOUSE, P. J. *Stress-Strain Relationships in Yarns Subjected to Rapid Impact Loading. Part X: Stress-Strain Curves Obtained by Impacts With Rifle Bullets.* Textile Res. J., v. 33, 1963, p. 919.

9. SMITH, J. C., FENSTERMAKER, C. A., and SHOUSE, P. J. *Stress-Strain Relationships in Yarns Subjected to Rapid Impact Loading. Part XI: Strain Distributions Resulting from Rifle Bullet Impact.* Textile Res. J., v. 35, 1965, p. 743.

10. PARKER, J. P., and KEMIC, C. S. *A Flywheel Impact Test for Measuring Physical Properties of Tire Cords.* High-Speed Testing, v. III, Interscience, New York, 1962, p. 3.

11. LYNCH, F. deS. *Dynamic Response of a Constrained Fibrous System Subjected to Transverse Impact. Part II: A Mechanical Model.* Army Materials and Mechanics Research Center, AMMRC TR 70-16, July 1970.

12. RECHT, R. F. *Response of Backing Materials to Ballistic Impact.* Paper presented to Ad Hoc Committee on Personnel Armor Materials, National Research Council, Natick, Massachusetts, February 13, 1968.

13. MOORE, W. J. *Physical Chemistry.* Prentice-Hall, Inc., New York, 1950, p. 495.

14. PAULING, L. *The Nature of the Chemical Bond.* Third Edition, Cornell University Press, Ithaca, New York, 1960, p. 85.

15. BROUTMAN, L. J., and McGARRY, F. J. *Fracture Surface Work Measurements on Glassy Polymers by a Cleavage Technique. I. Effects of Temperature.* J. Appl. Polymer Sci., v. 9, 1965, p. 589.

16. HALL, I. H. *The Effect of Strain Rate on the Stress-Strain Curve of Oriented Polymers. I. Presentation of Experimental Results.* J. Appl. Polymer Sci., v. 12, 1968, p. 731.

17. SHEEHAN, W. C. *Fibers for Personnel Armor.* Article appearing in The Development of Lightweight Armor. Report prepared by Ad Hoc Committee on Personnel Armor Materials Advisory Board on Military Personnel Supplies, as a service of The National Academy of Sciences to the U. S. Army Natick Laboratories, under Contract No. DAAG-17-68-C-0163, September 1968, p. 61.

UNCLASSIFIED
Security Classification

DOCUMENT CONTROL DATA - R & D

(Security classification of title, body of abstract and indexing annotation must be entered when the overall report is classified)

1 ORIGINATING ACTIVITY (Corporate author)	2a. REPORT SECURITY CLASSIFICATION
Army Materials and Mechanics Research Center Watertown, Massachusetts 02172	Unclassified
	2b. GROUP

3 REPORT TITLE

DYNAMIC RESPONSE OF A CONSTRAINED FIBROUS SYSTEM SUBJECTED TO TRANSVERSE IMPACT

PART I: TRANSIENT RESPONSES AND BREAKING ENERGIES OF NYLON YARNS

4 DESCRIPTIVE NOTES (Type of report and inclusive dates)

5 AUTHOR(S) (First name, middle initial, last name)

Anthony F. Wilde, John J. Ricca, Lonnie M. Cole, and Joseph M. Rogers

6 REPORT DATE	7a. TOTAL NO. OF PAGES	7b. NO. OF REFS
November 1970	36	17

8a. CONTRACT OR GRANT NO	9a. ORIGINATOR'S REPORT NUMBER(S)
b. PROJECT NO D/A 1T062105A329	AMMRC TR 70-32
c. AMCMS Code 502E.11.295	9b. OTHER REPORT NO(S) (Any other numbers that may be assigned this report)
d. Agency Accession Number DA OB 4752	

10 DISTRIBUTION STATEMENT

This document has been approved for public release and sale; its distribution is unlimited.

11 SUPPLEMENTARY NOTES	12. SPONSORING MILITARY ACTIVITY
	U. S. Army Materiel Command Washington, D. C. 20315

13 ABSTRACT

The effects of high-speed transverse missile impact upon textile yarns were observed by high-speed photography in a study of the transient behavior of a series of nylon 6/6 yarns differing systematically in mechanical properties. The loss in missile kinetic energy was determined directly from the reduction in missile velocity. The shape of these energy loss curves was due to the partition of missile energy into yarn kinetic energy and yarn strain energy. Estimates were made of the yarn breaking strains for these impact tests. The effects of yarn tenacity and impact velocity (strain rate) upon the impact behavior of these yarns were discussed and compared to their static behavior. Comparisons were also made with the effect of strain rate upon the breaking energies of nylon yarns reported in the literature. (Authors)

DD FORM 1 NOV 68 1473 REPLACES DD FORM 1473, 1 JAN 64, WHICH IS OBSOLETE FOR ARMY USE.

UNCLASSIFIED
Security Classification

KEY WORDS	LINK A		LINK B		LINK C	
	ROLE	WT	ROLE	WT	ROLE	WT
Fibers						
Nylon yarns						
Impact						
Deformation						
Velocity						
Tensile strength						
Strains						
Wave propagation						
Strain rate						
Transient response						
High-speed photography						
Kinetic energy						
Tensile modulus						
Failure						
Lightweight armor						